*Estuarine, Coastal and Shelf Science* (2002), **55,** 829–856
doi:10.1006/ecss.2002.1032

# Estuarine Physical Processes Research: Some Recent Studies and Progress

**R. J. Uncles**

*Plymouth Marine Laboratory, Prospect Place, The Hoe, Plymouth PL1 3DH, U.K.*

*Received 1 October 2001 and accepted in revised form 1 May 2002*

The literature on estuarine physical studies is vast, diverse and contains many valuable case studies in addition to pure, process-based research. This essay is an attempt to summarize both some of the more recent studies that have been undertaken during the last several years, as well as some of the trends in research direction and progress that they represent. The topics covered include field and theoretical studies on hydrodynamics, turbulence, salt and fine sediment transport and morphology. The development and ease-of-application of numerical and analytical models and technical software has been essential for much of the progress, allowing the interpretation of large amounts of data and assisting with the understanding of complex processes. The development of instrumentation has similarly been essential for much of the progress with field studies. From a process viewpoint, much more attention is now being given to interpreting intratidal behaviour, including the effects of tidal straining and suspended fine sediment on water column stratification, stability and turbulence generation and dissipation. Remote sensing from satellites and aircraft, together with fast sampling towed instruments and high frequency radar now provide unique, frequently high resolution views of spatial variability, including currents, frontal and plume phenomena, and tidal and wave-generated turbidity. Observations of fine sediment characteristics (floc size, aggregation mechanisms, organic coatings and settling velocity) are providing better parameterizations for sediment transport models. These models have enhanced our understanding both of the estuarine turbidity maximum and its relationship to fronts and intratidal hydrodynamic and sedimentological variability, as well as that of simple morphological features such as intertidal mudflats. Although few, interdisciplinary studies to examine the relationships between biology and estuarine morphology show that bivalve activity and the surface diatom biofilm on an intertidal mudflat can be important in controlling the erosion of the surface mud layer.


**Keywords:** Estuaries; tidal rivers; morphology; stratification; turbulence; turbidity; instrumentation; observations; numerical models; theory; wavelets

## Introduction and background

This essay attempts to summarize some of the more recent studies on estuarine physical processes which, from a personal viewpoint, are thought to be particularly important to the development of the topic. Experimental field studies and theoretical or numerical studies are summarized separately and graphical illustrations utilize independent, generally unpublished data from measurement campaigns in the Tamar and Tweed Estuaries, U.K., in order to emphasize the general applicability of some of the findings. The articles covered are relatively new; usually they have been published within the last several and mainly the last 5 years, although some reference is given to older research. Dyer (1997, 1986), Lewis (1997) and Officer (1976) give syntheses of much of the earlier work in their textbooks, along with explanations and illustrations of many of the concepts involved.

The quantitative study of estuarine dynamics began with the work of Pritchard (1956, 1954, 1952), in which he delineated the tidally averaged momentum balance of the James River estuary and highlighted the pivotal role of the density (or buoyancy or gravitational) current — the so-called estuarine circulation. That work led to many of the studies that have since guided estuarine research. Despite the importance of the conceptual framework that Pritchard initiated, a striking feature of much of the more recent work has been its shift in focus away from mean conditions and towards the influence of tidal variability and turbulence on estuarine dynamics. This has been due partly to an increased awareness of the importance of non-linear phenomena and partly to the recognition that, in many estuaries, periodicity in the strength of stability caused by tidal stirring, winds and waves can lead to an alternation between periods of strong

E-mail: rju@pml.ac.uk

0272–7714/02/120829+28 $35.00/0

stratification and strong mixing. The stratification-destratification cycle acts, in turn, as an important physical control on the local environment and its productivity. There has also been increasing awareness that suspended particulate matter, SPM, which includes suspended sediment and which often exhibits strong intratidal variability, can significantly supplement thermohaline stratification and water column stability, especially in the near-bed boundary layer of turbid estuaries.

The classic formulation of estuarine circulation in partially mixed (partially stratified) estuaries (i.e. Hansen & Rattray, 1965), as well as more recent formulations, assume a rectangular channel cross-section. In reality, transverse depth variations are an obvious feature of most natural estuaries and generate important hydrodynamic features due, in part, to frictional and density differences between shoals and channels (e.g. Huzzey & Brubaker 1988). Increased attention has been concentrated on the transverse distributions of both density and along-estuary mean flow since Fischer's (1972) suggestion that these played a crucial role in estuarine mass transport. In the past, efforts to measure this transport sometimes led to extremely labour-intensive, multi-station field studies (e.g. Kjerfve & Proehl, 1979). The transverse velocities themselves, which complete the three-dimensional velocity field, have, however, generally been neglected. Advances in instrumentation, such as the acoustic Doppler current profiler, ADCP, the ocean surface current radar, OSCR (Prandle & Ryder, 1985) and airborne and space-borne technology have greatly facilitated the observation of transverse variability and spatial variations in general.

Estuarine frontal systems appear to be ubiquitous and have been studied qualitatively, if not always quantitatively, for more than 20 years. Airborne remote sensing of fronts has added a new dimension to our visualization and appreciation of their nature (e.g. Ferrier & Anderson, 1997*a*, *b*). Brown *et al.* (1991) presented widespread examples of convergence lines in several estuaries of the U.K. and Largier (1992) reviewed much of the work on tidal intrusion fronts. Most of this work indicates that density gradients are essential to the development of fronts, although some recent ADCP measurements have provided high resolution spatial data on convergence cells that develop under almost homogeneous conditions.

Whether the process of interest is frontal, large-scale circulatory, or the result of switching stratification on or off, it is clear that a central requirement is to understand the processes that control vertical structure and the diffusion of properties through the water column. To achieve this understanding and apply it to prediction, it is necessary to solve the dynamical equations and to incorporate the controlling interactions between vertical fluxes and water column stratification. The requirement here is for an appropriate closure scheme for the mixing, several of which are available and most of which involve an explicit representation of turbulent kinetic energy and its dissipation (e.g. Luyten *et al.*, 1996). This interaction of turbulence, stratification and shear has been the focus of numerous laboratory, numerical and observational studies in the open ocean, but until recently there were few data for shallow, energetic estuaries.

The detailed processes affecting salt transport integrate temporally and spatially to determine the salinity intrusion length and large-scale density gradient in an estuary. On long time-scales, the down-estuary advection of salt due to river outflow is balanced by up-estuary salt fluxes due to spatial and temporal correlation of velocity and salinity. A great deal of work has been completed on this topic over the last 30 years and Lewis (1997) and Smith and Scott (1997) have reviewed much of this. Nevertheless, it is an important topic and there is still ongoing work, most of which is concerned with case studies for particular estuaries.

It has been appreciated for many years that a number of different mechanisms may be responsible for the formation and maintenance of the estuarine turbidity maximum, ETM, depending on tidal energy, morphology and stratification conditions (Dyer, 1986; Postma, 1967). In partially mixed estuaries, the most commonly cited mechanism for maintaining an ETM is the convergence of near-bed flow close to the limit of salt intrusion due to estuarine circulation, although much of the recent work has identified other, more complex accumulation mechanisms. Numerical modelling has greatly aided the study of these processes, although model development requires parameterizations for several complex sedimentological phenomena, some of which are far from understood despite the existence of relatively new measurement techniques based on optics and acoustics. Partly in response to this uncertainty there has been more attention paid to the characteristics of fine sediment trapped within the ETM, especially its aggregation and settling behaviour, as well as the transverse and vertical spatial variability that occurs within it.

An ambitious objective for estuarine researchers is the prediction of estuarine morphology. Mean sea level is currently estimated to rise by approximately 0·5 m during the 21st century (from the average of scenario model runs: IPCC, 2001; Leatherman, 2001). It is important to know how an estuary, its intertidal areas and its salt marshes will respond to this

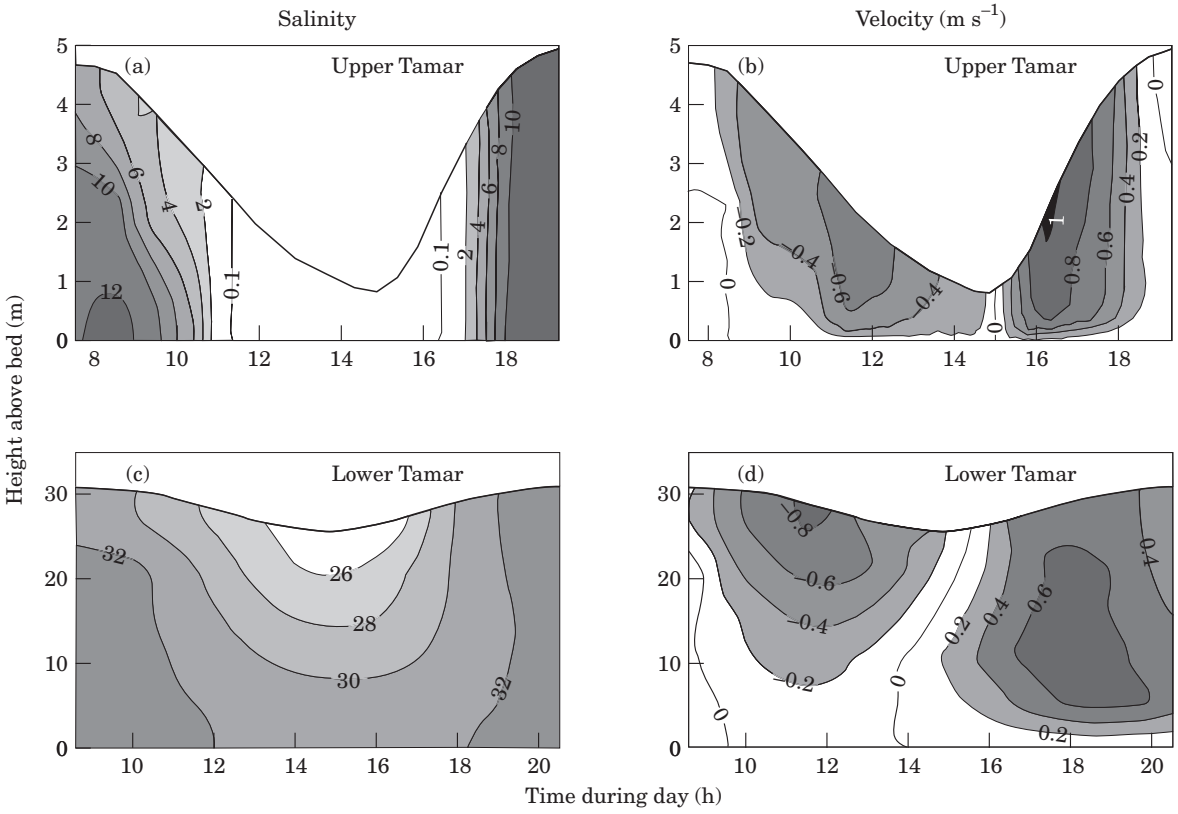


FIGURE 1. Illustration of the effects of tidal straining on the vertical profiles of spring tide salinity distributions at stations in the upper and lower Tamar Estuary, U.K., and the causative tidal currents (flood positive). In the upper Tamar, (a) and (b), tidal straining causes the fresher, surface isohalines to be preferentially advected down-estuary during the ebb leading to strong stratification (as illustrated schematically in Figure A1 of the Appendix) until the freshwater-saltwater interface passes through the station, (a). During the flood, decreasing straining, strong currents and large near-bed shears, (b), generate mixing and the isohalines become nearly vertical, (a). In the much deeper lower Tamar, (c) and (d), tidal straining leads to greatest stratification around low water (LW), (c). The associated currents, (d), clearly illustrate the combined influence of the gravitational (estuarine) circulation and tidal flow, with peak near-surface and near-bed current speeds during the ebb being faster and slower, respectively, than those during the flood.

increase in sea level. Recent advances in morphology tend to have resulted from mathematical and numerical modelling, validated by short-term intensive measurements. However, it is becoming clearer that many of the parameterizations used in the sediment transport modules of these models, such as erosion thresholds (e.g. McAnally & Mehta, 2001; Mehta, 1993) are not simply physics-dependent, but are influenced to a greater or less extent by biological-physical interactions. A very important feature of newer research has been the incorporation of these biological effects into sediment transport studies.

## Fieldwork studies

### *Hydrodynamics of vertical processes*

Whereas in the past emphasis has often been on mean (subtidal, residual or tidally averaged) conditions through the water column, in recent years much more attention has been given to intratidal behaviour. This has been aided by observations in regions of freshwater influence (ROFIs). Observations in the Rhine region of the North Sea (Simpson & Souza, 1995) showed evidence of large semidiurnal oscillations in water-column stratification at times of reduced mixing. The amplitude of these semidiurnal variations, which was of the same order as the mean stratification, resulted primarily from the interaction of cross-shore tidal-current straining with the density gradient[A1] (see Figure A1 in the Appendix). The comparable magnitudes of amplitude and mean stratification frequently resulted in the water column being almost vertically mixed once per tide.

The same phenomena are even more pronounced within estuaries (illustrated for the Tamar Estuary in Figure 1). In the Hudson River estuary, and also in the upper reaches of the Tamar [Figure 1(a)], tidal

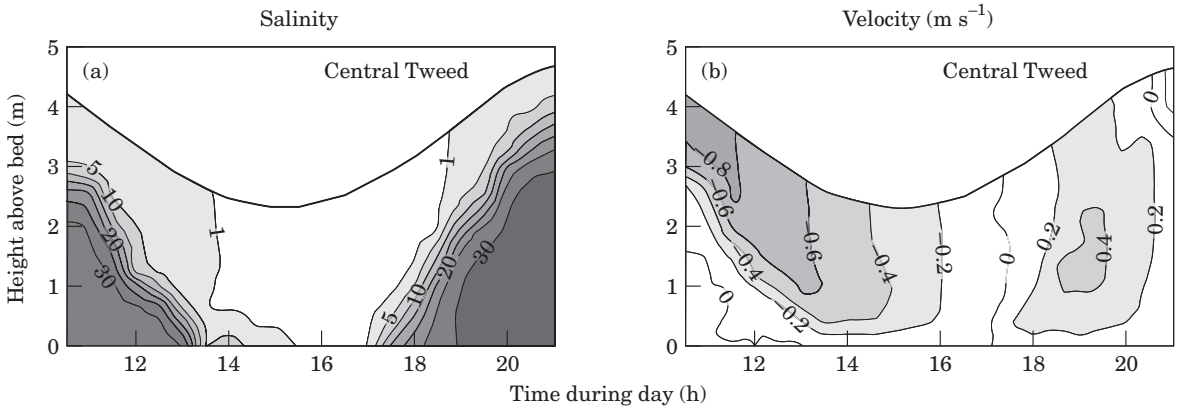


FIGURE 2. Illustration of tidal variations in the pycnoline position and associated current structure (flood positive) during neap tides and moderate runoff in the central Tweed Estuary, U.K. Vertical movements of the pycnocline, (a), largely reflect down-estuary advection of the salt wedge by ebbing tidal currents and subsequent up-estuary advection during the flood. Changes in pycnocline thickness are not large, indicating that it has grown sufficiently wide to achieve a measure of dynamic stability. During the ebb, the low salinity (<5) upper layer has an almost uniform fast speed (i.e. low shear), (b), and the saline wedge (>30) moves very slowly and with little shear. Almost the entire current shear is restricted to the pycnocline layer. During the flood, there is much less shear in the pycnocline and maximum speed is reached within it at peak flood, (b). Near-bed shear is greater during the flood than the ebb when the pycnocline is present.

straining maintained stratification during the ebb, while it promoted the growth of a uniform, near-bed mixed layer during the flood (Nepf & Geyer, 1996). In general, maximum and minimum near-bed stratification occurred during late ebb and late flood, respectively [as in the lower Tamar, Figure 1(c)], reflecting the dominant role played by tidal straining in determining intratidal variations. Stacey *et al.* (2001) have argued that even the estuarine circulation might be partially caused by barotropic (water level driven) forcing in the presence of this flood-ebb stratification asymmetry. Other measurements, again in the Hudson, further emphasized the importance of intratidal variability (Geyer *et al.*, 2000). Estimates of vertical eddy viscosity[A2] indicated that there was significant tidal asymmetry in which flood values exceeded ebb values by a factor of two, so that the vertical structure of tidally averaged stress differed greatly from that deduced from the tidally averaged shear[A2]. Even without the influence of buoyancy, a pronounced tidal current asymmetry, in which flood speeds significantly exceed ebb speeds, is a common feature in the upper reaches of many strongly tidal estuaries [Figure 1(b)]. The influence of spring-neap variations on tidal straining was explored by Sharples *et al.* (1994). They observed vertical density structure in the Upper York River estuary that showed periods of mixed and stratified conditions in which reduced stratification, or complete mixing, occurred during strong spring tidal currents and significant stability during weaker currents.

In strongly stratified estuaries (illustrated for the Tweed Estuary in Figure 2), tidal variations in stratification are reflected in the depth and thickness of the density interface between surface and bed layers (Cudaback & Jay, 2000). Earlier work predicted the interface depth using inviscid (zero viscosity, zero friction) two-layer theory, in which baroclinic (density driven) estuarine circulation was combined with the barotropic tidal current (Helfrich, 1995). In reality, bottom friction and interfacial mixing are usually non-negligible in many shallow estuaries (Farmer & Armi, 1986; Pratt, 1986). Cudaback and Jay (2000) therefore used a bulk Richardson number criterion[A3], in conjunction with two-layer model results, to estimate the depth and thickness of the pycnocline. They found that bottom friction increased vertical shear on the ebb and decreased it on the flood, so that the pycnocline grew thicker on the ebb because of greater shear instabilities and thinner on the flood, consistent with their field measurements.

In many shallow estuaries there is a mid-depth maximum in flood currents because these are driven by an along-channel barotropic pressure gradient that is constant with depth and a baroclinic pressure gradient that increases monotonically towards the bed, where friction is strong. This feature is strikingly exhibited by flooding currents in both the partially mixed Tamar and the stratified Tweed [Figures 1(d) and 2(b)] as well as the stratified Columbia (Cudaback & Jay, 2001). Cudaback and Jay (2001) explored this effect for the Columbia River entrance channel using a simple three-layer model and simulated their observed currents, including the mid-depth maximum in flood currents, to within approximately 10%.

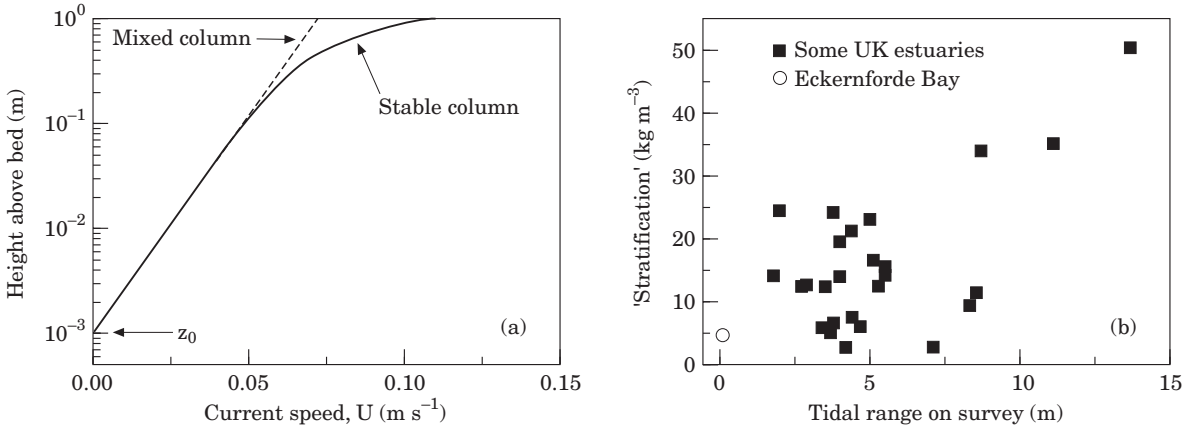


FIGURE 3. Although the presence of a pycnocline and strong stratification have very obvious influences on estuarine circulation [e.g. Figure 2(b)], less pronounced thermohaline and SPM stratification may also have important consequences for the circulation and near-bed tidal mixing. In the low tidal energy Eckenförde Bay, (a), a bed to surface density difference of only approximately 4 kg m$^{-3}$ in 25 m of water produces a marked convexity of the near-bed log profile. Currents must be substantially faster some distance above the bed in a stable water column than in a mixed column to exert the same bed shear stress for an equivalent roughness length, $z_0$. Although increased near-bed shear in strongly tidal estuaries will reduce this stability effect, these are often highly turbid systems and potentially able to generate large SPM stratification, (b). Observations of the maximum bed to surface density difference in numerous UK estuaries at times close to HW of spring tides, (b), illustrate pronounced stable stratification. At low tidal ranges, density differences due to salinity of >20 kg m$^{-3}$ can occur, whereas at high tidal ranges the density differences due to SPM can be >30 kg m$^{-3}$.

The onset and variability of estuarine density stratification has many consequences for water and sediment transport and ecology (e.g. Joordens *et al.*, 2001; Boicourt, 1992). Thermohaline stratification may influence the near-bed velocity profile in low to medium energy estuaries and other systems influenced by buoyancy. Using near-bed velocity measurements from Eckernförde Bay, Friedrichs and Wright (1997) have shown that the empirical fitting of data to classical, 'law of the wall' log profiles[A4] (e.g. Sanford & Lien, 1999) may lead to large overestimates of bottom stress and roughness length if thermohaline stratification is neglected [Figure 3(a)]. In a similar study of South San Francisco Bay, broadband ADCPs were used to make detailed measurements of the turbulent mean velocity distributions within 1·5 m of the bed (Cheng *et al.*, 1999). Faster current speeds led to a reduction of roughness length[A4], which they hypothesized to be due to sediment erosion. Within energetic estuaries, SPM eroded from the bed sediments by strong currents may cause density stratification [Figure 3(b)] and influence the stability of the water column. Winterwerp (2001) illustrated this phenomenon using a 1-D (one-dimensional) numerical model of the water column to simulate a catastrophic collapse of turbulence following the formation of fluid mud layers. Despite the fact that there has been much work on the role of circulation patterns in accumulating fine sediment within estuaries, no work seems to have been done on the inverse process, in which suspended sediment may potentially affect the large-scale circulation. Alvarez *et al.* (1999) demonstrated that sediment-load effects on the depth averaged tidal dynamics of a bay system were likely to be small, but the consequences for mean circulation in highly turbid, stratified estuaries may be much more significant.

Although tidal mixing and its competition with buoyancy forces (ultimately derived from freshwater runoff and perhaps assisted by surface heating) are known to be important processes in estuaries, much less consideration has been given to the influence of waves. It is known that salt marshes, which occur in many temperate estuaries, can very efficiently dissipate incident wave energy (Möller *et al.*, 1999) and wave effects are likely to be non-negligible for all but the smallest and most sheltered of estuaries. In coastal regions sheltered from the direct impact of swell and storm-wave activity, Pattiaratchi *et al.* (1997) have shown that locally generated wind waves, particularly those associated with strong sea-breeze activity (where this occurs) play a dominant role in controlling nearshore and foreshore processes. Waves will also play a role in estuarine plume regions (Figure 4) and in large estuaries, where they may influence sediment and mixing processes in shallow subtidal and intertidal areas (Green & MacDonald, 2001; Ruhl *et al.*, 2001; Christie *et al.*, 1999; Green *et al.*, 1997). In very shallow areas, such as over intertidal mudflats and within coral reef lagoons, even small breaking waves

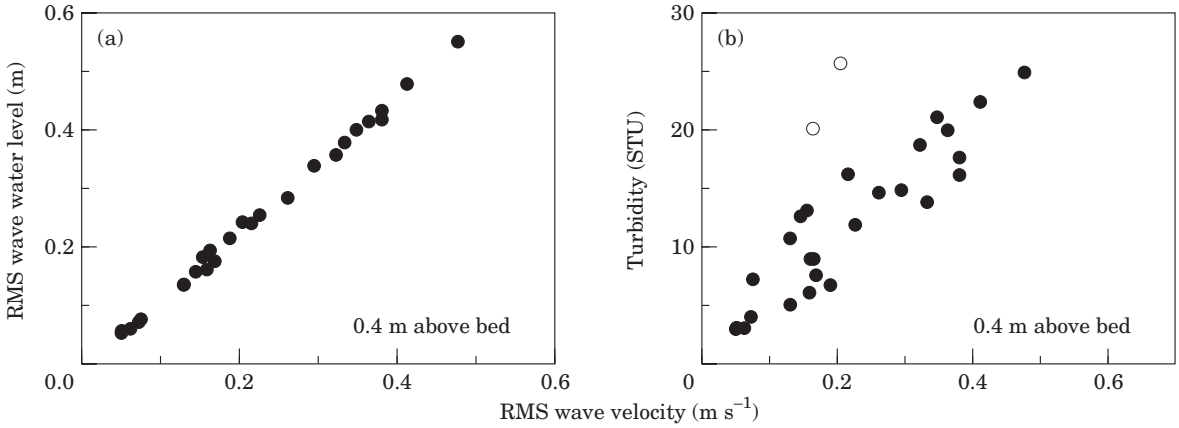


FIGURE 4. Illustration of the strong correlation between surface wave water level fluctuations and their associated velocities at 0·4 m above the bed, (a), and between these velocities and turbidity at the same height, (b), in the coastal plume region of the Tweed Estuary. The site was located approximately 1 km offshore of its mouth in 11·5 m of water. Plotted data are root mean squares (RMS) of the wave variables, which are then tidally averaged to produce a synthesis of behaviour (one data point in (a) and (b) per tidal cycle for each of many tides). The STU (siltmeter turbidity units) correspond to mg l$^{-1}$ (10$^{-3}$ kg m$^{-3}$) of SPM for the optical backscatter calibration obtained using silt and clay suspensions. When strong wave activity occurs prior to or during flood tides, relatively high SPM loads are advected into the estuary. The two open data points in (b) correspond to periods of moderate wave activity but very high runoff and sediment discharge from the Tweed into its coastal zone. At that time the ebb-tide plume comprised waters of less than ambient salinity and higher than ambient turbidity (e.g. Blanton *et al.*, 1997).

appear to be capable of enhancing local turbidity [Plate 1(A)].

*Hydrodynamics of transverse processes*

The effects of channel shape on cross-estuary (i.e. transverse or lateral) spatial variations in the along-channel (longitudinal or axial) velocity are known to be significant in partially mixed estuaries (Friedrichs & Hamrick, 1996). Strong lateral variations occur in the Tamar Estuary close to high water (HW) when currents on the flanking shoals begin to ebb before those in the main channel (Figure 5).

Observations made across a 6·5-km wide section of the James River estuary indicated that density-induced circulation was the dominant contribution to along-channel mean velocity, although river runoff also provided a measurable velocity (Friedrichs & Hamrick, 1996). Another feature that occurs in the transverse dynamics of this partially mixed estuary is fortnightly (spring-neap) variability. Valle-Levinson *et al.* (2000*a*) used a towed ADCP over approximately 4 km-wide sections (which featured a channel flanked by shoals) to investigate this aspect of the transverse momentum balance[A5]. They showed that transverse baroclinic pressure gradients were larger during neap than spring tides and that, during springs, advective accelerations were predominantly greater than Coriolis accelerations, especially over the edges of the channel.

The picture is more complicated on intratidal time-scales, for which sharp lateral spatial gradients can occur at certain stages of the tide (Figure 5). Valle-Levinson and Atkinson (1999) have shown that similarly strong spatial gradients can occur even in the flow through very wide estuaries. They utilized ADCP data from the lower Chesapeake Bay to illustrate bathymetrically induced spatial gradients in the currents. The greatest transverse shears and convergence zones were found on the shoulders of the channel, where bathymetric changes were sharpest. Longitudinal tidal currents can also generate transverse circulation patterns (secondary flows) as they respond to the curvature of a meandering channel. These secondary flows are particularly persistent in the presence of stable density stratification ($R_i$>0·25)[A6] when the effects of vertical mixing and friction are greatly reduced (Lacy & Monismith, 2001).

Wind affects the flow patterns within estuaries and has been quantified at the mouth of the Delaware (Wong & Moses-Hall, 1998) and at the Chesapeake Bay entrance (Valle-Levinson *et al.*, 1998). Valle-Levinson *et al.* (1998) found that most of the subtidal (tidally averaged, or, more correctly, tidal low-pass filtered) volume exchange took place in the main channels. Gravitational circulation and wind forcing produced the mean flow patterns in the channels, regardless of wind direction, whereas the flow over shoals was caused by tidal rectification (a non-linear

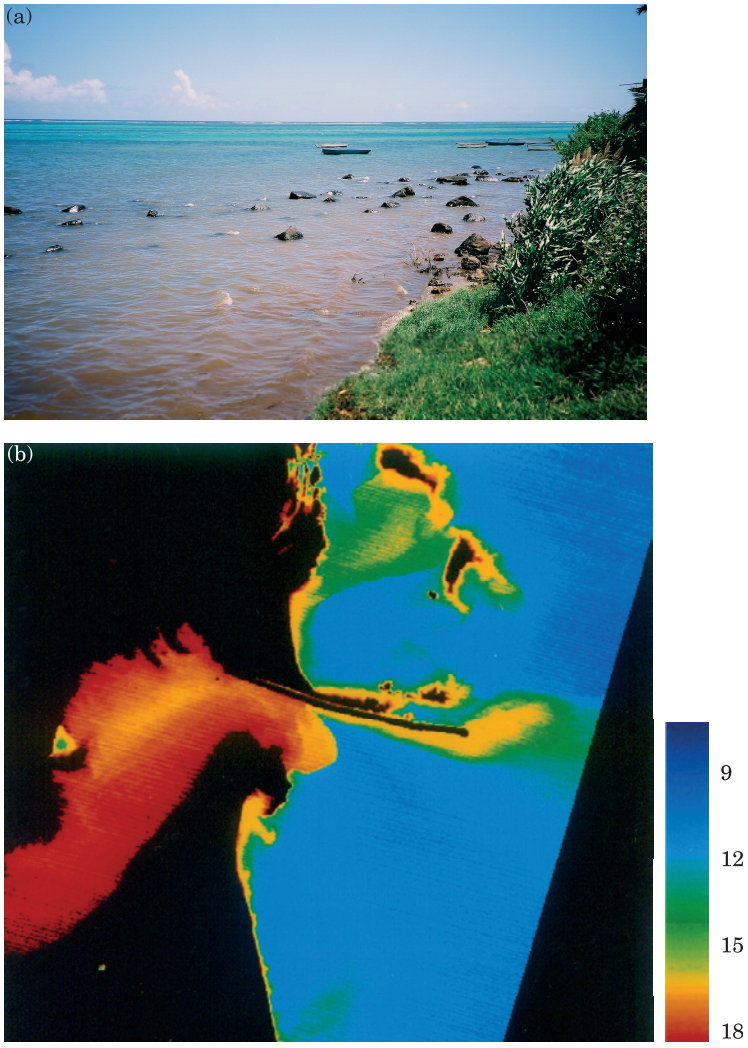


PLATE 1. Even small amplitude waves that break at the leading edge of a rising tide as it floods over a very shallow and low-sloping intertidal area, (1A), are able to generate enhanced turbidity in the presence of fine sediment. The depth in the near-shore area of this coral reef lagoon (Mauritius) is less than 0·5 m. The waves were estimated visually to be about 2–3 m long and to have periods of 1–2 s. The sources of fine sediment are local coastal soil erosion and nearby river inputs during cyclones. Airborne remote sensing, (1B), can provide high-resolution views of sea surface variability that are particularly valuable when sharp spatial gradients occur. This image shows the surface temperatures associated with a tidal intrusion front that propagated through the Tweed Estuary's inlet on a flooding, mean-range tide at LW+3·1 h. The data were derived from a Daedalus-AADS-1268, Airborne Thematic Mapper (ATM) thermal band 11 image, and calibrated using simultaneous sea-truth measurements. The initial frontal system (at LW+2·1 h) appears to have been triggered by an inflow Froude Number transition at the neck of the inlet. The occurrence of a critical inflow Froude Number then led to the plunging of cool, coastal surface waters (blue) beneath warm, estuarine surface waters (red) at the neck of the inlet.

tidal processes analysed by Li & O'Donnell, 1997) and wind forcing, with the dominating influence determined by wind direction. Wind affects have also been observed at the entrance to a shallow, semi-arid coastal lagoon (the Bay of Guaymas in the Gulf of California, Valle-Levinson *et al.*, 2001). Subtidal currents over the shoals were driven in the same direction as the wind stress, whereas a return flow occurred in the deep channel, as would be anticipated for a system dominated by barotropic forcing and bed friction. In small, shallow estuaries the effects of winds can lead to large changes in residence time, according to whether the wind forcing is either delaying or progressing the transport of freshwater from river to coastal plume (Geyer, 1997).

The ADCP, together with airborne and satellite remote sensing and other modern instrumentation has greatly aided our observation and understanding of three-dimensional, spatial variability in estuaries. Detailed maps of surface tidal, wind-driven and other

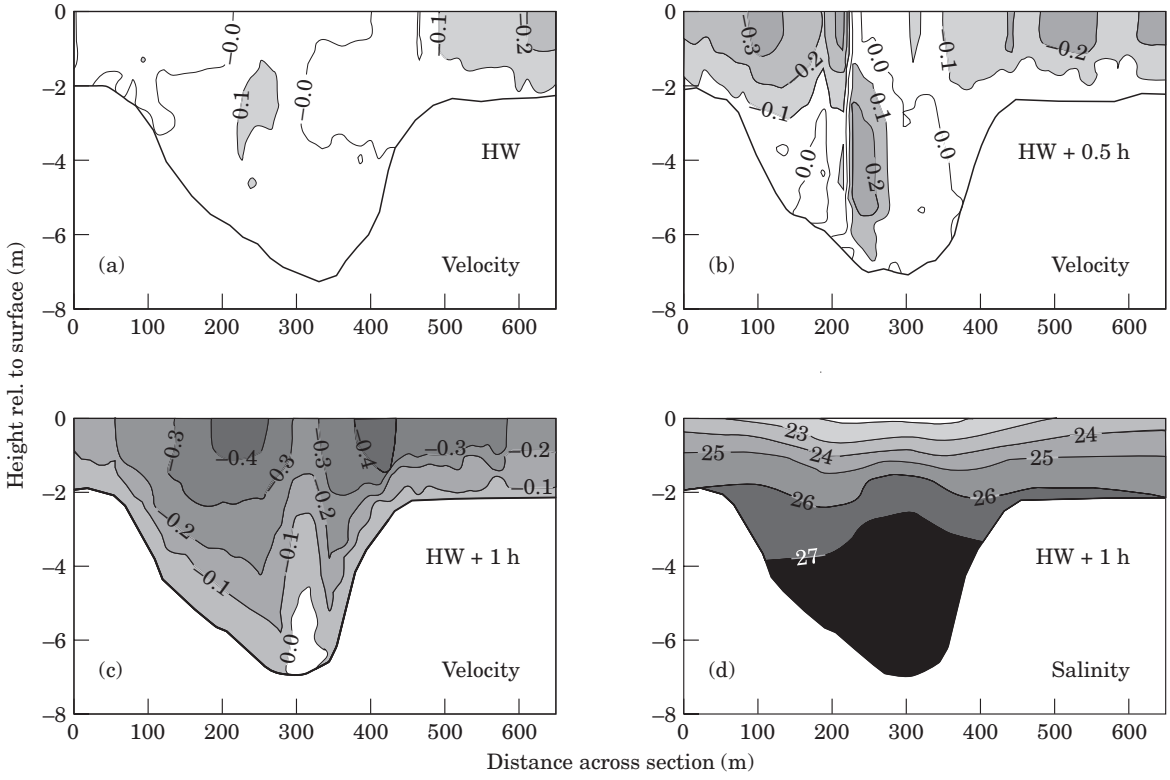


FIGURE 5. Spatial distribution of longitudinal currents (flood positive) across a 650-m-wide section of the central Tamar Estuary (looking up-estuary) during spring tides. Data were obtained using an ADCP deployed with typical horizontal and vertical resolutions of 10 and 0·1 m, respectively. At HW the current was already ebbing slowly over the intertidal shoals, with faster currents flowing near the banks, (a), whereas much of the main channel water was still slowly flooding. The ebb currents had increased in speed by HW+0·5 h, (b), although a central core of flooding water remained in the main channel, where a zone of intense lateral shear developed between it and the ebbing water to the west (left). Relatively fast ebb currents occurred in the upper 2 m and over the shoals by HW+1h, (c), forming two ' jets ' located over, and either side of, a deep core of slowly flooding water. These features are the result of enhanced density-driven flows in the channel and enhanced frictional drag over the shoals, and lead to the picture of mean currents depicted in Figure A1 of the Appendix. The salinity distribution at HW+1 h, (d), was obtained during a different but similar spring tide and relies on just five stations located over the section. Nevertheless, it does demonstrate a ' doming ' of salinity (>27) in the channel, corresponding to the flooding core in (c), and two ' bulges ' of lower salinity (<23) near-surface waters, corresponding to the two ' jets ' in (c).

currents in the coastal zone have been derived from HF (high frequency) ocean surface current radar (OSCR; Davies *et al.*, 2001; Shen & Evans, 2001; Prandle, 1997*a*). However, because the spatial resolution of HF radar is of order 1 km, these systems are only appropriate for larger estuaries. Even with this technology the complexity of transverse variability confounds our attempts to experimentally quantify the transport of SPM and solutes from estuaries to the coastal zone. As an illustration, an observational programme in the Mersey Estuary, U.K., used the following array of instruments to measure currents (Lane *et al.*, 1997): bottom mounted and towed ADCPs, bottom and (floating) platform-mounted electromagnetic current meters, and moored rotary meters. The observations extended over a spring-neap cycle and included near continuous, half-hourly towed ADCP transects across the 1·5-km-wide Mersey Narrows. Despite the scale of this observational programme, and state-of-the-art instrumentation, it was concluded that net fluxes to the coastal zone could not be determined by direct measurements when they were less than a few percent of the oscillatory tidal fluxes.

Provided only near-surface data are required then satellite and airborne remote sensing provides a unique view of spatial variability that may be invaluable to studies of estuarine and coastal water quality [Plate 1(B)]. Pattiaratchi *et al.* (1994) used multi-date Landsat Thematic Mapper data to show that great confidence may be placed in image predictions (i.e. estimates of water-borne variables) obtained using empirical algorithms and that these data therefore offered a cost-effective tool for complementing regular monitoring programmes. The AVHRR (advanced

very high resolution radiometer) has been used to study surface SPM patterns in San Francisco Bay at a resolution of approximately 1 km, demonstrating the role of waves in causing enhanced turbidity within shallow embayments (Ruhl *et al.*, 2001). Unfortunately, satellite spatial resolution is frequently too coarse for use in all but these larger estuaries. The resolution of SeaWiFS (sea-viewing wide field-of-view sensor) is again approximately 1 km, which makes it valuable for large estuaries and their plumes, but CrIS (cross-track infrared sounder) has a resolution of approximately 25 m, which will make it suitable for a wide range of studies. Airborne remote sensing operates from low flying light aircraft and has much greater spatial resolution (several metres or less). It utilizes instrumentation such as the ITRES Compact Airborne Spectrographic Imager (CASI) and the Airborne Thematic Mapper (ATM). The SLFMR (scanning low-frequency microwave radiometer, Goodberlet *et al.*, 1997) is capable of remotely sensing salinity.

### *Estuarine frontal processes*

Flow convergence leading to density front formation is a common phenomenon within estuaries and has been studied for many years, although modern instrumentation and airborne remote sensing have greatly aided our visualization and understanding of the processes at work [e.g. Plate 1(B)]. These frontal systems can take many forms, both longitudinal and transverse, and can include non-density-driven convergence zones such as those occurring within Langmuir cells, which are driven by wind-current, wave-current interactions (Nimmo Smith & Thorpe, 1999). Other examples, which are density dependent, are the tidal intrusion front and the ' axial ' (or longitudinal) convergence front (e.g. Dyer, 1997). The former is often associated with a topographical feature such as a sill or width constriction [as in Plate 1(B)], which then acts as a control on the flow via an inflow Froude number[A7]. The latter is driven by the tidal straining of isohalines resulting from transverse variations in flow[A1], which then set up transverse density gradients that drive longitudinal frontal convergence zones (see Figure A1 in the Appendix).

ADCPs have been used to study the frontal structure associated with the up-estuary propagation of a salt wedge as the density and tidal currents ' push ' the fresher, surface waters back into the James River estuary (Brubaker & Simpson, 1999). They have also been used to study the head of the buoyant, gravity current outflow plume from the Connecticut River estuary (O'Donnell *et al.*, 1998) and Chesapeake Bay (Marmorino & Trump, 2000). Marmorino and Trump found that the inflow of plume waters into the head was confined to a narrow (2 m deep) surface layer and that frontal propagation was supercritical relative to this layer (i.e. Froude number >1)[A8].

Valle-Levinson *et al.* (2000*b*) used an ADCP to measure velocity profiles across a section of the James River estuary that was characterized by a main and secondary channel separated by relatively narrow shoals. Transverse surface flow convergence zones appeared over the edges of the channels and were produced by the phase lag of the channel flow relative to that over the shoals (e.g. Figure 5). Flood convergence zones developed close to HW and those on the ebb appeared soon after maximum currents. Most of these convergence zones caused fronts in the density field as well as flotsam lines that appeared over the edges of the channel and lasted <2 h. The transverse flows associated with convergence zones were mostly in the same direction throughout the water column and were proportional to the tidal amplitude and channel steepness. Results indicated that the convergence zones were produced mainly by the tidal flow interacting with the channel-shoal bathymetry, i.e. they did not appear to require the presence of density gradients, although they became stronger once density gradients had formed.

### *Turbulence*

Significant advances have been made in our quantitative understanding of estuarine and coastal turbulence over the last few years, largely due to developments in profiling instrumentation such as FLY (fast, light yo-yo), MSS (microstructure measuring system, Kocsis *et al.*, 1999) and SWAMP (shallow water microstructure profiler).

Some measurements in coastal ROFIs and regions of thermal stratification also have relevance to estuaries. The free-fall FLY profiler has been used to determine the variation in turbulent energy dissipation[A9] through the water column over a semidiurnal tidal cycle at mixed and stratified sites in the Irish Sea (Simpson *et al.*, 1996). Dissipation exhibited a strong quarterdiurnal variation and had a pronounced phase lag that increased with height above the bed. This quarterdiurnal signal extended throughout the water column in mixed conditions, whereas it was confined to about 40 m above the bed in the summer stratified situation, with phase delays of more than 4 h relative to the bed. Qualitatively, these are features that would be anticipated for a semidiurnal tide in which tidal current speeds maximize twice per tide, when much of the production and dissipation of turbulent energy

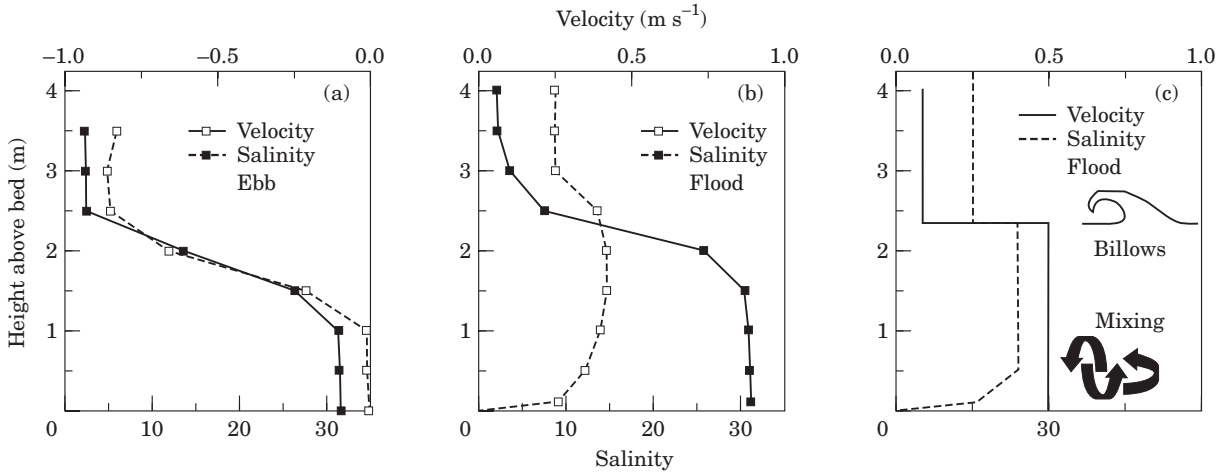


FIGURE 6. Examples of ebb, (a), and flood, (b), salinity and velocity profiles (flood positive) in the Tweed (for times 11:30 and 19:30h, respectively, in Figure 2) and a schematic, (c), showing the mixing processes. The lines drawn between plotted data points are for visualization only. Bottom-layer mixing, (c), results from current shear at the bed (tidal ' stirring '). Pycnocline mixing at the unrealistically sharp halocline, (c), results from Kelvin–Helmholtz (K–H) shear instabilities (' billowing '). Evaluating the bulk Richardson number for the observed interface[A3] indicates that the pycnocline is essentially stable (i.e. $R_{ib}$>0·25) in (a) and (b) and for much of the tide when the salt wedge is present. The evaluation uses a constant density gradient, constant shear layer approximation for the pycnocline, as analysed by Turner (1973), and ignores the finite thickness of the surface and bed layers. According to Turner's (1973) analysis, the sharp interface, (c), will always be unstable to K–H billows for perturbations of a scale that will be encountered in a real estuary. The hypothesized sharp interface between coastal and river waters is likely, therefore, to rapidly spread vertically by billowing and turbulent mixing (Cisneros-Aguirre *et al.*, 2001) until it reaches an equilibrium thickness.

occurs in the near-bed region of intense shear. Profiling observations in a coastal ROFI by Ripeth *et al.* (2001) showed similar intratidal, ' tidal straining ' salinity variations to those observed in estuaries (Figure 1). At this location, turbulent energy dissipation had a quarterdiurnal signal in the lower water column and a semidiurnal signal in the upper column, due to the reduced stratification and much greater mixing that occurred on the flood [illustrated for salinity in Figure 1(a,c)]. The same phenomena of bed-generated turbulence, upward mixing and subsequent suppression in the presence of a density-interface (e.g. the halocline—which may itself become unstable) also occur in shallow estuaries [Figure 6(c)].

Peters and Bokhorst (2001) and Peters (1999, 1997) observed turbulent mixing, stratification and currents in the Hudson River estuary using the free-falling SWAMP and a 600-kHz ADCP. The progression from neap to spring tides caused a severe reduction in stratification from an initial top-to-bottom salinity difference of 18 to <4, consistent with Sharples *et al.*'s (1994) York River estuary data. Small gradient Richardson numbers[A6] ($R_i$) were restricted to the weakly stratified bottom layer on the flood portion of neap tides but occurred throughout the water column during the late ebb of springs. Turbulent dissipation rates varied approximately as $R_i^{-1}$ and, as a result, neap-tide turbulent mixing was intense only in the bottom layer during the flood, with weak mixing in the central halocline [e.g. Figure 6(a,b)]. During spring tides, strong mixing occurred that extended throughout the water column during the latter part of the ebb. These periods of intense mixing showed increasing phase lag with distance from the bed, consistent with Simpson *et al.*'s (1996) Irish Sea data. Values of $N_z$ and $K_z$[A2] maximized at $1–5 \times 10^{-2}$ m$^2$ s$^{-1}$, and minimized in the pcynocline at $10^{-5}$($K_z$) and $10^{-4}$ ($N_z$) m$^2$ s$^{-1}$ (Peters & Bokhorst, 2001).

Trowbridge *et al.* (1999) used other types of instrumentation to make near-bed turbulence measurements in the Hudson. The relationship between bed stress and velocity gradient was not consistent with the ' law of the wall ' during the ebb, but was consistent within approximately 1 m of the bed during the flood [as in Figure 3(a) for the homogeneous, mixed column] although not at greater heights. Local stratification was thought to be too small to explain this effect, which was possibly due to a reduction of the turbulent length scale[A10] by the finite thickness of the relatively mixed layer beneath the pycnocline [e.g. the bottom layer in Figure 6(c)].

Observations of turbulence have also been made in the partially mixed northern San Francisco Bay estuary. Vertical profiles of Reynolds stress[A11] were measured directly using an ADCP, which again illustrated that energetic turbulence was confined to a

bottom mixed layer by overlying stratification (Stacey *et al.*, 1999). Comparisons of Reynolds stress, Richardson number and turbulent Froude number[A10] showed that the water column could be divided into regions based on the relative importance of buoyancy effects. The observed water motions appeared to be buoyancy-affected turbulence, rather than internal waves, although the turbulent Froude numbers were <1 in much of the upper water column at times, indicating strong effects due to stratification and buoyancy.

Measurements of interfacial turbulence and mixing have been made under conditions of moderate river-flow and neap tides in the highly stratified Columbia River estuary [Kay & Jay, in press (a)]. Mixing along the top of the salt wedge was found to occur only during the ebb at the measurement site. This mixing coincided with periods of supercritical internal Froude number[A8] and precluded a ' quasi-equilibrium ' view of the salt wedge in which tidal effects were confined to small longitudinal and vertical variations in wedge position. The turbulent Froude number was observed to be close to unity, indicating interplay between shear and buoyancy effects. Estimates of the partition of energy dissipation between bed-generated and internal mixing [e.g. Figure 6(c)] showed that internal mixing accounted for about two thirds of the total turbulent kinetic energy produced in the salt reach of the Columbia [Kay and Jay, in press (b)].

### *Horizontal salt transport processes*

Although large-scale salt intrusion in estuaries has been studied experimentally for decades, the availability of 3-D (three-dimensional) numerical models has greatly aided our understanding of these integrated phenomena by permitting a spatially detailed view of the simulated salt transport, salinity gradients and tidal processes. Using numerical models and analyses, Bowen (1999) demonstrated theoretically that salt transport is increased dramatically during stratified periods when vertical mixing is weak. Analysis of observed salt transport in the Hudson River estuary confirmed this prediction and showed that stratified periods of enhanced estuarine salt transport occurred in five-day intervals once a month during apogean neap tides (when the moon lies farthest from the earth's centre of attraction). Despite this, the salt balance adjusted very little to the spring-neap modulation of salt transport, but adjusted rapidly to pulses of freshwater runoff. Presumably, this occurred because the time scales associated with salt mixing were much longer than those associated with salt advection by the runoff.

When large-scale SPM, salt (or other solute) transport is analysed in a tidally averaged sense, rather than instantaneously, certain key, long-term processes can often be identified. Geyer and Nepf (1996) showed that tidal pumping of salt[A12] was important in a moderately stratified estuary. Based on measurements of velocity and salinity at several cross-sections in the Hudson, tidal pumping was found to be larger than the up-estuary salt flux due to the estuarine circulation (the shear contribution[A12]) during high runoff, but relatively insignificant during low runoff. Strong tidal pumping during high runoff conditions was caused by large vertical excursions of the halocline that correlated with tidal flow. Time-series measurements of velocity and salinity have similarly been used to demonstrate the importance of salt fluxes caused by tidal pumping within the strongly tidal Conwy Estuary, North Wales (Simpson *et al.*, 2001). Both shear and pumping components of the salt transport are important in the central reaches of the partially mixed Tamar Estuary (Figure 7).

### *Fine sediment dynamics*

An estuarine turbidity maximum (ETM) is often observed in the upper reaches of turbid estuaries and many studies have focused on this important phenomenon (e.g. ERF15, 2001; Sanford *et al.*, 2001; Wolanski *et al.*, 1996). Much of the recent work has identified tidal pumping of SPM as an important accumulator of fine sediment (illustrated for salt in Figure 7). Pumping results from the correlation between tidal currents and concentration, which may be due, e.g., to flood-ebb differences in sediment erosion and deposition, or from the consequences of flood-ebb asymmetry in stratification or mixing (Figure 1, Chant & Stoner, 2001; Geyer *et al.*, 2001; Le Hir, 2001). As might be anticipated, there is a pronounced spring-neap variability in fine sediment pumping within strongly tidal estuaries (Guézennec *et al.*, 1999). Most of the work has treated the ETM as a longitudinal feature with little attention given to transverse variability, although transverse variations have been observed (Figure 8).

The Hudson has an ETM zone in the intermediate-salinity portion of the salinity intrusion (Geyer *et al.*, 1998). The ETM is skewed toward the west side of the estuary, which is significantly shallower than the east side and is subject to rapid accumulation of soft, unconsolidated sediment, in contrast to the east side which has lower suspended loads and a hard bed of coarse sediment. Velocities and SPM concentrations in the region reach 1·3 m $s^{-1}$ and 2 kg $m^{-3}$, respectively (Orton & Kineke, 2001). A 3-D numerical

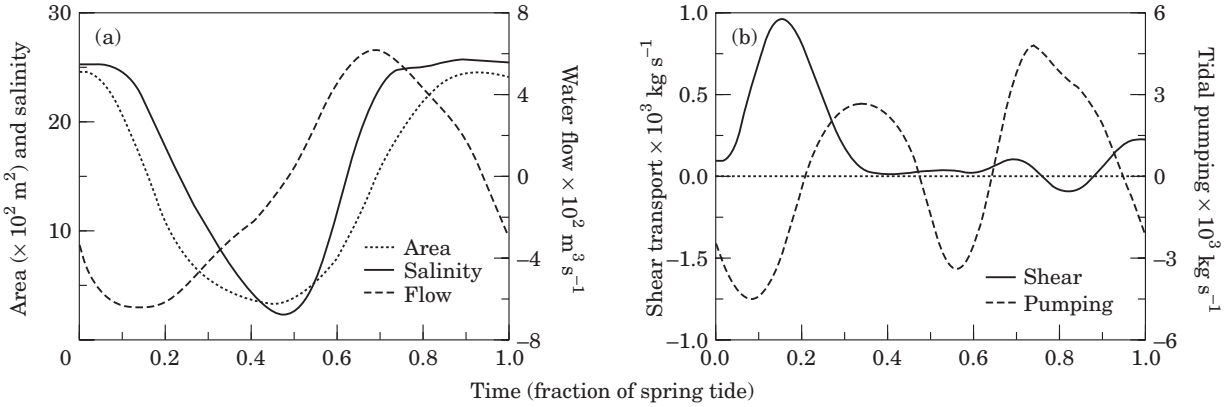


FIGURE 7. The bulk estuarine salt transport through a cross-section and over a tidal cycle depends on contributions from the residual water flow, tidal pumping and shear[A12]. The intratidal variations in cross-section area, section-averaged salinity and water flow (flood positive) through the section, (a), are illustrated for the central Tamar during a moderate runoff, spring tide. The non-zero correlation between the instantaneous water flow and salinity leads to tidal pumping when averaged over a tide. The amplitude of the intratidal variations in the product of flow and salinity are an order of magnitude greater than the tidally averaged pumping (4500, (b), as opposed to 290 kg s$^{-1}$ of salt transport). The salt shear term is almost always positive and has a tidally average transport of 190 kg s$^{-1}$, compared with a peak value on the early ebb of 950 kg s$^{-1}$. These correspond to a dispersion coefficient[A12] of 120 m$^2$ s$^{-1}$, of which the pumping contributes 70 and the shear 50 m$^2$ s$^{-1}$.

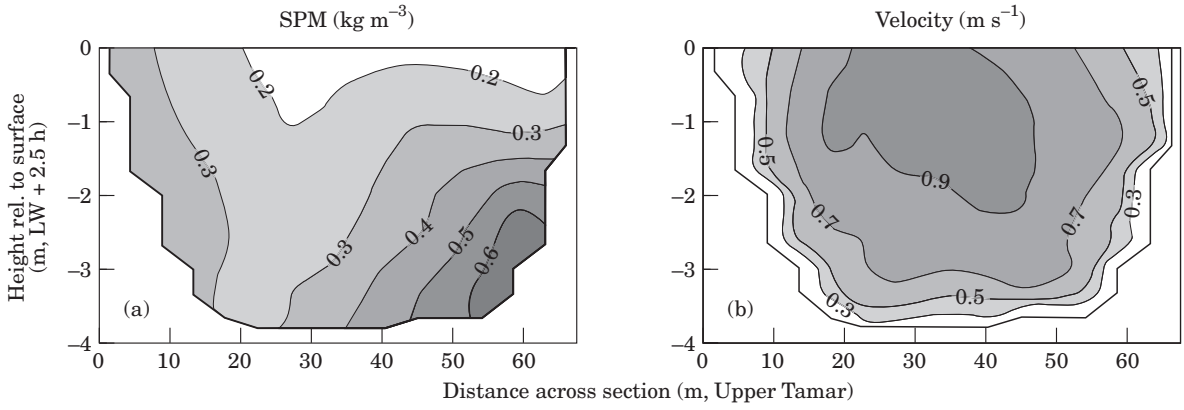


FIGURE 8. Cross-sectional distributions (looking up-estuary) of suspended particulate matter concentration, SPM, and longitudinal velocity (flood positive) at HW-2·5 h during a moderate runoff spring tide in the upper Tamar Estuary. The contours are based on just four stations located across the section, but nevertheless illustrate the pronounced transverse spatial variations in SPM, (a), and longitudinal velocity, (b), that occur over this ' U ' shaped section. The LW depth at large spring tides is <1 m in the deepest part of the section, which is scoured of erodible fine sediment during strong flood and ebb current speeds. The lower intertidal banks act as deposition zones during the very shallow, slow ebb flows that occur over them prior to their uncovering. This material is then eroded and suspended as fast flowing flood currents cover the banks.

model identified two mechanisms for trapping sediment (Geyer *et al.*, 1998), a lateral convergence due to transverse, baroclinically driven flow during the flood and a convergence of flow due to the formation of a longitudinal salinity front during the ebb.

Much less information is available for SPM behaviour in highly stratified estuaries. The Columbia is a salt-wedge system that, over as little as tens of metres (Orton *et al.*, in press), can change from highly stratified estuary to well-mixed river. SPM concentrations and settling rates can also rapidly change over this transition. Fain *et al.* (in press) investigated seasonal and tidal-monthly SPM dynamics in the Columbia using acoustic backscatter (ABS) and velocity data in or near the ETM. The ETM in the Columbia, like in many other estuaries, migrates seasonally in near-unison with the salt intrusion (e.g. Grabemann & Krause, 2001; Kappenberg & Grabemann, 2001; McManus, 1998). Four characteristic settling velocity classes were defined from Owen Tube measurements (e.g. Dearnaley, 1997) and an inverse analysis used to determine the contribution of

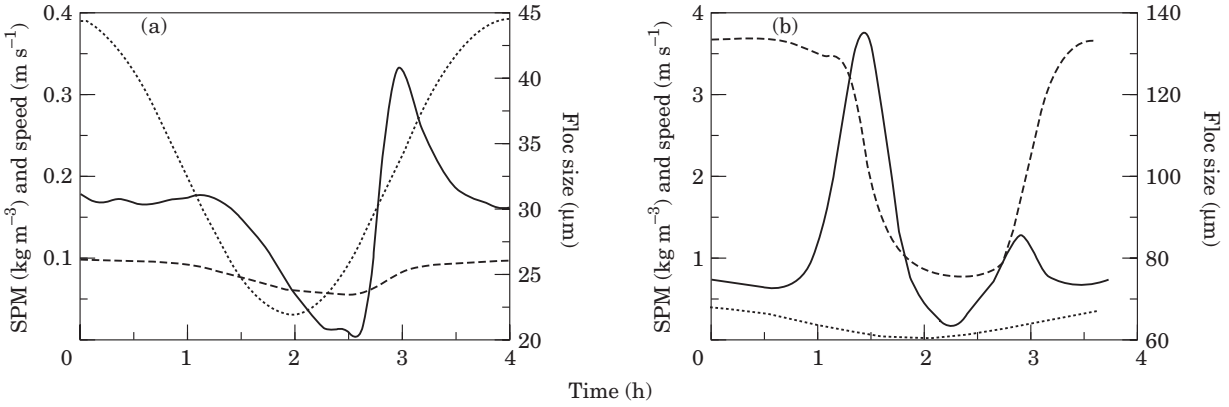


FIGURE 9. Experimental results on the aggregation of natural estuarine suspended sediment under controlled conditions in an annular flume. The flume was programmed to simulate oscillatory tidal currents. The size distribution of suspended particles was measured in-situ using a Lasentec P-100 laser-reflectance particle size instrument, with the sensing probe inserted directly through the wall of the flume. The flume was filled with river water collected up-estuary of the Tamar's ETM and a bulk sample of mobile surface sediment was taken from a mud bank within the ETM. Various quantities of this stock sediment were added to the flume to provide SPM concentrations of nominally 0·1 kg m$^{-3}$, (a), and 4 kg m$^{-3}$, (b). The flume was run through consecutive, 4-h cycles in which the mean current velocity varied sinusoidally from 0·05 to 0·45 m s$^{-1}$, (a) and (b). Eroded SPM concentration maximized at around maximum current speeds and minimized shortly (<0·5 h) after minimum speeds. Floc size varied by a factor of approximately two throughout the speed and SPM cycles and was much greater within the higher turbidity environment, (b). – – –, SPM; · · · ·, speed; ——, size.

the four classes to each observed SPM profile. Non-dimensional parameters were defined to investigate how river flow and tidal forcing affected particle trapping. Results indicate that the most effective particle trapping occurred during neap tides with low to moderate runoff. Fortnightly variations in SPM, characterized by low concentrations during neap tides and high concentrations during springs appeared to result from a residual, up-estuary transport of near-bed sediment during the neap tide [Kay & Jay, in press (b)]. At that time the reduced ability of the flow to suspend material into the upper part of the water column (where it could have been flushed from the estuary) coupled with very small, near-bed currents during the ebb, appeared to result in a net up-estuary transport of flocculated SPM. During springs, mixing into the upper part of the flow resulted in flushing of SPM to the coastal zone.

Insights into ETM formation and other fine sediment phenomena have been aided by increased understanding of suspended particle characteristics, obtained using modern instrumentation such as the LISST-100 (laser in-situ scattering and transmissometry, Gartner *et al.*, 2001) for particle size determination and INSSEV (*in situ* settling velocity, Dyer & Manning, 1999). The settling rates of fine-grained particles, and in particular the aggregated particles (flocs) that generally constitute the bulk of ETM suspended sediment depend on the suspension's size distribution (e.g. Hill *et al.*, 2000), which in turn depends predominantly on velocity shear and SPM concentration within the water column (Figure 9). Laboratory measurements by Bale *et al.* (in press) have shown that enhanced aggregation of estuarine particles occurs under conditions of high concentrations of SPM and intermediate conditions of current velocity and turbulent shear (Figure 9). Bale *et al.* (in press), Manning and Dyer (1999), Dyer and Manning (1999) and Lick *et al.* (1993) have derived empirical expressions between floc diameter, SPM and turbulent velocity shear[A9]. At the highest experimental shears, Bale *et al.* found that there appeared to be an asymptotic floc size that reflected the existence of very strong microflocs (usually defined to be <100 μm in size and largely bound by organic materials such as polysaccharides, van Leussen, 1994). These controlled experiments complement results from field surveys, which also exhibit strong temporal variability in floc sizes within highly turbid estuaries (Law *et al.*, 1997), and which indicate that flocs with a median diameter of 500 μm or larger can form within very high particle concentration suspensions under low shears.

Polysaccharide polymers (extra-cellular polymeric substances, EPS) produced by benthic diatoms and other organisms that inhabit intertidal mud in estuaries are known to exert a strong influence on the stability of the sediment by increasing the threshold for erosion (Paterson *et al.*, 2000). Although tentative, much of the polymer material appears to be flushed

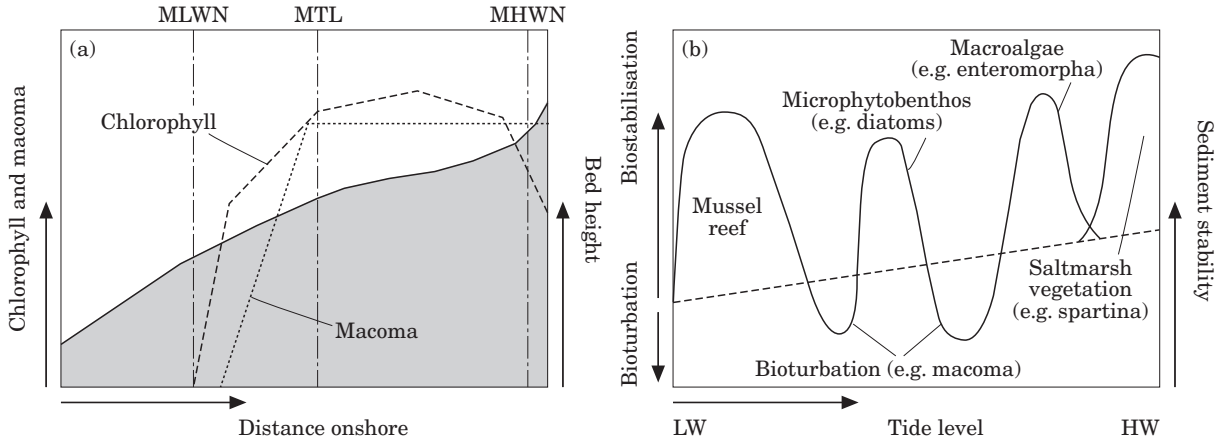


FIGURE 10. Schematic to illustrate how the erosion properties of intertidal mudflats may depend on a balance between the physical and biological processes of stabilization and destabilization. Microphytobenthos (such as benthic diatoms) enhance stability. If this variable is parameterized in terms of its chlorophyll component, (a), it may be represented in very approximate terms as increasing up the intertidal mudflat from the mean low water neap (MLWN) line. A maximum in chlorophyll is reached that, in this illustration, lies between the mean tide level (MTL) and mean high water neap level (MHWN). A population of the bioturbating small clam, *Macoma balthica*, on the other hand, destabilizes the sediment, and is shown in (a) as increasing up the mudflat to reach a plateau at the higher levels. A generalized schematic, (b), shows an overall increase in sediment stability progressing up the mudflat from LW to HW over the salt marsh (if present), with localized enhanced stability due to a mussel reef, microphytobenthos, macroalgae and saltmarsh vegetation. Localized reduced stability results from the presence of bioturbating clams.

out of the intertidal mud during tidal inundation. If so, it may then act as a source of organic material for the surfaces of suspended particles, thereby influencing their ability to aggregate with other particles.

### *Morphology*

There has been a surge of interest in estuarine morphology over the last few years that has led to the publication of numerous articles on the behaviour of intertidal mudflats and renewed attempts to seek a classification scheme that encompasses their morphological variability (Dyer, 2000; Dyer *et al.*, 2000). As in other areas, instruments such as the PEEP (photoelectronic erosion pin) system (Lawler *et al.*, 2001), CSM (cohesive strength meter, Tolhurst *et al.*, 1999) and ‘ Sea Carousel ’ (Amos *et al.*, 1997) have facilitated remote monitoring of mudbank and mudflat erosion and their morphological responses to spring-neap and seasonal cycles. However, given the importance of morphological prediction in the context of climate change, very little research has been undertaken into medium space and time scales (kilometres and years). Much of the existing research is directed at physical and sedimentological processes using short-term intensive experiments, with little work on longer term monitoring to observe seasonal and inter-annual weather and climate influences on tidal processes and sediment fluxes. Just as regrettable, there have been relatively few interdisciplinary studies to examine the relationships between biology and morphology.

What measurements have been made to correlate measured erosion properties and biological characteristics of intertidal mudflats show the importance of the surface diatom layer (biofilm) in modifying the initial erosion of the surface mud layer (Anderson, 2001; Paterson *et al.*, 2000; Riethmüller *et al.*, 2000). Widdows (2001) has taken this concept of ‘ bio-sedimentology ’ further and hypothesized that the erosion properties of cohesive, intertidal mudflats depend on a balance between the physical and biological processes of stabilization and destabilization. Bio-stabilization of sediments is effected by several variables. These include the density of microphytobenthos, algal mats, higher plants (such as sea grass and salt marsh vegetation), tube-building polychaetes (spionid worms) and biogenic reefs, such as mussel beds (Figure 10). The potential for macrophyte beds to reduce local current speeds, increase accretion and reduce turbidity has been reviewed by Madsen *et al.* (2001). Bio-destabilization mainly results from the bioturbation caused by burrowing and deposit-feeding animals, such as bivalves, polychaetes and crustaceans. Anderson (2001) found that biofilms were absent where macrofaunal populations were dominant, thereby enhancing the peak-and-trough nature of erodibility across the mudflat [Figure 10(b)], and that the faecal pellet content of the bed also influenced

rates of sediment erosion. In low energy estuarine environments, Wright *et al.* (1997) demonstrated that benthic animals can profoundly affect the subtidal (meaning submerged in this context) sediment balance, with lowest erosion thresholds coinciding with the most intense mixing of the sediment column by bioturbation activity.

## Theoretical and numerical studies

### *Hydrodynamics of vertical processes*

Models and theoretical analysis have played an important role in enhancing our understanding of estuarine physical processes. This is particularly true when observations have isolated a specific phenomenon, such as tidal straining and its relationship to stratification, which may then be investigated through the application of models. A numerical model that employed the Mellor-Yamada (MY) level 2 turbulence closure scheme[A13] was used to investigate water column stability in the Upper York River estuary (Sharples *et al.*, 1994). This model highlighted the need to resolve the depth-dependence of horizontal density gradients in order to reproduce the observed spring-neap behaviour of water-column stratification.

Simple models of vertical structure in stratified tidal flows have also produced insights into the details of mixing in shallow estuaries. Monismith and Fong (1996) considered two methods of generating vertical mixing in their 1-D (vertical) model of the water column. Shear instability resulted in bed-induced turbulence (tidal stirring) as well as shear-layer turbulence derived from the top of the bottom mixed layer [Figure 6(c)], both of which caused deepening of the mixed near-bed layer by entraining lower density waters from the upper water column.

The importance of waves in modifying bed shear stresses and in numerous other oceanographic phenomena has led to much theoretical work (e.g. Shaowu *et al.*, 1998; Mei *et al.*, 1997) and the development of several wave models. One such model is WAVEWATCH (Tolman & Booij, 1998) although the physical processes included in this model do not take into account conditions where the waves are severely depth-limited, which is the situation most likely to apply in many estuaries. Another model of greater application to estuaries is SWAN (simulating waves near-shore), which is a third-generation wave model that computes random, short crested, wind-generated waves in coastal and inland waters (Ris *et al.*, 1999).

### *Hydrodynamics of transverse processes*

Models of current and density structure over estuarine cross-sections have proved to be useful in isolating the various processes that generate this structure and in indicating the level of process-complexity that needs to be incorporated into the models. The transverse structure of along-channel mean velocity over a nearly triangular cross-section of the James River estuary was found to be primarily due to the density-driven circulation, modified by local depth variations (Friedrichs & Hamrick, 1996). Comparisons of analytical and observed tidal velocity amplitudes and phases over their chosen cross-section indicated that linear models needed to incorporate across-channel variations in eddy viscosity, such as a power-law dependence on local depth.

Li and Valle-Levinson (1999) applied a 2-D (two-dimensional) analytical tidal model to a narrow estuary of arbitrary transverse depth variations. Provided the transverse variation of tidal water level was small, then tidal wave propagation was essentially 1-D and directed along the estuary, regardless of the depth distribution. The tidal velocity, however, had a strong transverse shear and was generally three-dimensional. Tidal current speeds and depths were highly correlated, such that fastest, along-channel tidal speeds occurred in the deepest water (also strikingly illustrated by Cheng *et al.*, 1993, using a 2-D hydrodynamic model). Phases of the along-channel velocity in shallow water led those in deeper water, which resulted in a delay of flood or ebb in the channel relative to the shallow regions (illustrated in Figure 5 for the Tamar). Transverse (cross-estuary) velocities were generally slow in the middle of a channel, but reached maximum speeds over the edges of bed slopes.

### *Turbulence*

Advances in turbulence modelling have accompanied advances in techniques to measure turbulence in the sea and estuaries and have reached the stage where effects due to breaking surface waves are being incorporated (Burchard, 2001a; Mocke, 2001), although considerable uncertainties remain. For example, the lowest levels of turbulent energy dissipation ($\sim 10^{-5}$ W m$^{-3}$) measured in the Irish Sea pycnocline (Simpson *et al.*, 1996) were much greater than those predicted by a Mellor-Yamada level 2 closure scheme (MY2.0) model[A13]. However, when allowance was made for the diffusion of turbulent kinetic energy (with appropriate choice of diffusivity[A2]) the MY2.2 model satisfactorily simulated dissipation in

the stratified case. When diffusivity was set equal to vertical eddy viscosity (which depended on the Richardson number) the model underestimated dissipation in the pycnocline by two orders of magnitude, which implied the possible existence of a mid-water source of turbulent kinetic energy.

The Mellor-Yamada level 2.5 closure scheme[A13] (MY2.5) has been applied to turbulence observations in the partially mixed northern San Francisco Bay estuary (Stacey *et al.*, 1999). The model tended to underestimate turbulent kinetic energy in regions of strong stratification, where the turbulence was strongly inhomogeneous, and to overestimate turbulent kinetic energy in weakly stratified regions. It was thought that the underestimation was due to an inaccurate parameterization of turbulence self-transport (diffusion) from the near-bed region to the overlying stratification.

Considerable work has recently been undertaken on the parameterization of turbulence for use in numerical models and the associated computer codes have sometimes been made freely available. The GOTM (General Ocean Turbulence Model) code is an example (Burchard *et al.*, 1999). Comparisons of turbulence parameterizations are also available. Burchard *et al.* (1998) compared $k$–$\varepsilon$ and Mellor-Yamada two-equation turbulence models[A13]. The comparison between model results and field measurements of the rate of dissipation of turbulent kinetic energy for the stratified Irish Sea (Simpson *et al.*, 1996) showed that both models required modification through the inclusion of an internal wave parameterization if they were to correctly predict the observed turbulent dissipation. The stability functions that were used as proportionality factors in calculating the eddy viscosity and diffusivity[A13] had a stronger influence on the performance of the turbulence model than the choice of length-scale related equation. Burchard and Bolding (2001) have compared several other turbulence closure models for which the closure assumptions are contained within these stability functions.

### *Hydrodynamic models and theoretical techniques*

Great progress has been made in the development and application of numerical modelling techniques to estuarine and coastal waters over the last decade. Dyke (2001) has reviewed some of these techniques for 1-D, 2-D and 3-D time-dependent computer models. Although there are many examples of model applications, a particularly well validated 2-D model applicable to tidally dominated coastal plain estuaries and tidal lagoons has been presented by Cheng *et al.* (1993). Their model computed the detailed depth averaged tidal and density-driven circulation in San Francisco Bay, California. Results demonstrated the formation of wakes around islands and the changing phase differences between water levels and currents that occurred in the channels and over shoals as the tide propagated through the Bay.

The huge increase in personal computer (PC) power over the last decade has been a major driver in the application of these models. For example, a customized version of code originally developed at the Proudman Oceanographic Laboratory, U.K. (Holt & James, 2001) has been run on a PC to simulate the 3-D circulation and salt transport in the Tamar Estuary's coastal zone over a 1-year period (Siddorn *et al.*, in press). The model required approximately 3·5 days to run on a 43 × 68 × 20 (latitude, longitude, depth) grid using a single 1·4 GHz processor, Windows-based PC. Applications of these 3-D numerical models are now commonplace and they are routinely used for understanding processes within estuaries and adjacent coastal seas. Two models in common use that have been applied to estuaries are the Princeton Ocean Model (POM) and the Hamburg Ocean Primitive Equation Model (HOPE). Valle-Levinson and Wilson (1998) have used a series of 3-D numerical simulations to illustrate the effects of the Earth's rotation, tidal forcing and vertical mixing on water exchanges in an idealized estuary with sill bathymetry and in Long Island Sound. An unusual and well validated 3-D model that utilized harmonic expansions in time, rather than classical time stepping, and a spatial discretization based on triangular volume elements, rather than a regularly spaced grid of computational nodes, was applied to the Delaware Estuary by Walters (1997). His results illustrated the important effects of tidal straining and density stratification on the circulation, even during times of very low runoff and buoyancy input.

Advances in theoretical approaches have been made using wavelet transform tidal analysis methods (Flinchem & Jay, 2000; Jay & Flinchem, 1997). Continuous wavelet transforms are a relatively new technique that complement traditional Fourier analyses by providing interpretation for time-series data that are not statistically stationary or exactly periodic (e.g. river tides, Figure 11). Other approaches that are relatively novel to estuarine research include the utilization of data such as dissolved nutrients and salinity to generate over-determined sets of equations, which are then used to estimate estuarine circulation patterns (Gilcoto *et al.*, 2000), and neural network analysis for salinity prediction (Huang & Foo, 2002).

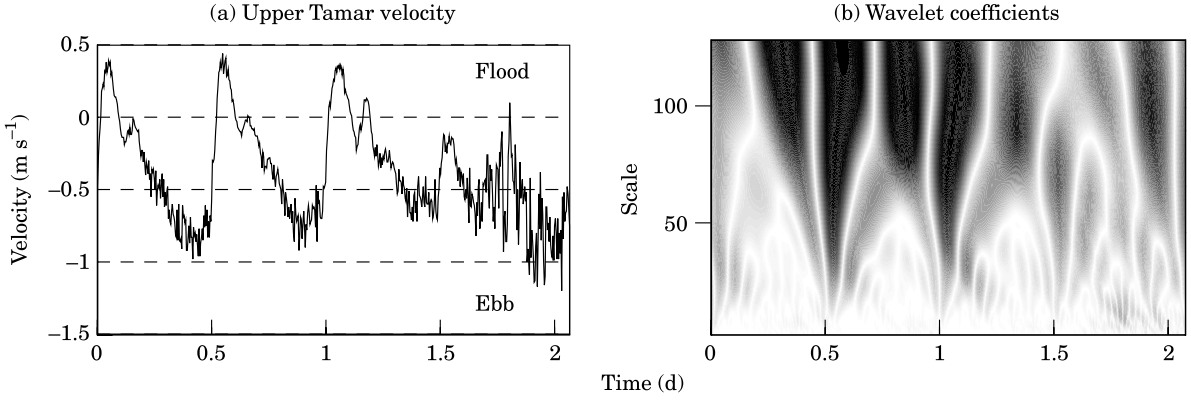


FIGURE 11. Time series of longitudinal velocity in the upper Tamar during moderate, increasing to high runoff, (a), and the wavelet scaling coefficients derived from it using a Daubechies (order 4) continuous wavelet transform (Burrus *et al.*, 1998), (b). A wavelet is a small wave of finite length that has its energy concentrated in time, as opposed to a sinusoid, which oscillates with equal amplitude for all time. Wavelets can be used in the series expansion of a transformed time varying signal in much the same way that sinusoids are used in Fourier series analysis. The velocity, (a), exhibits mainly semidiurnal variations and strong overtides (e.g. quarterdiurnal tides), together with high frequency variability. At approximately 1·5 days the runoff rapidly increased and the current became predominantly ebb-directed and extremely ' noisy '. The absolute magnitude of the wavelet scale coefficients (darkest regions show largest, most significant coefficients) exhibit broad, dark bands at large scales ($\sim$100). These correspond to the semidiurnal tides, which are eventually disrupted by strong runoff after 1·5 days. The branching at intermediate scales (<70) has the appearance of four ' arches ' that taken together extend over the whole period and widen down to the lowest scales. Each of these ' arches ' contains within its semidiurnal frame the darker banding corresponding to overtides (scales <50). The fine banding at small scales (<10) corresponds to high frequency variations. Banding associated with these variations is difficult to discern in this plot because of their small amplitude compared with the semidiurnal velocities. An exception is the darker banding at approximately 1·8 days for scales $\sim$10, which captures the greater high frequency variability exhibited by the time-series at this time, (a).

Hearn (1998) has presented a Stommel model[A14] description of a summer Mediterranean estuary (in which water exchange is controlled by density-driven processes) which appears to be the first detailed confirmation of the applicability of the Stommel model to estuaries. The Stommel model has two possible stable stationary states and it is shown that four types of steady state can characterize the estuary. They include the ' classical ' and ' inverse ' estuaries plus a solution, called ' quasi-neutral ', in which the estuary is close to neutrality but just marginally inverse. The fourth type of estuarine state is called ' intermittent ', which means that the estuary can relax to either the classical or quasi-neutral states.

### *Theoretical fine sediment dynamics*

Analytical models have been effective in enhancing our understanding of fine sediment dynamics in estuaries and the coastal zone. Prandle (1997*b*) used analytical theory to describe the tidal variability inherent in suspended sediment concentrations comprising clay, silt, and sand eroded by lunar and solar semidiurnal tidal currents. The associated 1-D (vertical) model involved only the ' particle ' fall velocity, the vertical-mixing coefficient (the eddy diffusivity[A2] for SPM—assumed constant) and the water's depth. For fast fall velocities the particles remained close to the bed and deposition occurred by advective settling, whereas for slow fall velocities the particles were well mixed vertically and settlement was more dependent on the assumed mixing coefficient.

Orton and Kineke (2001) have presented results from similar theoretical studies in which they compared observations of SPM concentrations (up to 2 kg m$^{-3}$) from the lower ETM of the Hudson with those calculated from a Rouse equation modified by stratification. When a well-defined pycnocline existed, cross-isopycnal mixing (modified by the gradient Richardson number[A6]) was strongly damped. Their analysis revealed that the two parameterizations most likely to account for differences between computed and measured SPM concentrations were those for settling velocity and stratification-induced water column stability. Best comparisons were obtained using a power law relationship for settling velocity, based on SPM concentration (e.g. Van Leussen, 1999; Krone, 1993; Mehta, 1993).

More complex applications of theory have included studies of the ETM. Friedrichs *et al.* (1998) used analytical methods to show that the tidally averaged, fine sediment transport pertinent to ETM formation in a strongly tidal, partially mixed estuary was due to three dominant effects in their equations. These were:

(i) flood-dominant tidal velocity asymmetry, (ii) down-estuary river flow, and (iii) settling/scour lag (the net longitudinal displacement of sediment ' particles ' over a tide resulting from the different conditions experienced by them during deposition and suspension) which was made effective by along-channel width convergence. The third ' width convergence ' effect represented a new insight into the mechanisms responsible for the maintenance of an ETM.

Numerical computer models have also been used to investigate ETM processes. Burchard and Baumert (1998) simulated an idealized, flat-bottom estuary in order to study the hydrodynamic control of the high turbidity zone by the combined influences of the salt intrusion and tidal movements. Their model was 2-D (depth-length) with high resolution in both time and space. After a few tidal periods the model exhibited a stable ETM at the up-estuary limit of salt intrusion. This trapping of SPM was due to a residual, near-bed, up-estuary transport in the region of the salt intrusion limit. Three physical causes for this effect were investigated: (i) gravitational circulation, (ii) tidal velocity asymmetry, and (iii) tidal mixing asymmetry. The first mechanism was related to the classical estuarine circulation. The second and third mechanisms were derived from the differences between the vertical profiles of velocity and SPM, respectively, during flood and ebb currents [related to the shear and pumping mechanisms illustrated for salt transport in Figure 7(b)]. For the idealized, strongly tidal estuary considered, both (i) and (ii) were necessary for the formation of an ETM, whereas (iii) affected the ETM only quantitatively, but not qualitatively, and appeared to be unnecessary for the existence of an ETM.

### *Theoretical morphology*

The simplest morphodynamic models concern the evolution of individual features such as tidal mudflats, sandflats or salt marshes. Approaches can range from analytical solutions of the simplified dynamical equations, to simple time-stepping predictions of surface elevation (height above a datum) using a few empirically-based parameters, as in recent salt marsh studies (van Wijnen & Bakker, 2001). The distribution of horizontal surface area with respect to elevation is termed hypsometry. Observations of tidal flat morphology have correlated convex (pointing upwards) hypsometry with large tide ranges, long-term accretion and (or) low wave activity. Concave hypsometry, in turn, has been correlated with small tide ranges, long-term erosion and (or) high wave activity.

Friedrichs and Aubrey (1996) demonstrated that this empirical variation in tidal flat hypsometry was consistent with a simple morphodynamic model that assumed tidal flats to be at equilibrium if maximum bed-shear stress were spatially uniform. This is equivalent to assuming that sediment is moved until the erosion threshold of the bed (taken to be constant) just exceeds the bed shear stresses everywhere on the tidal flat and movement ceases. Two general cases were considered: (i) dominance of maximum bed-shear stress by tidal currents and (ii) dominance by maximum wind-induced, wave-generated shear stress. Analytic solutions indicated that for a tidal flat which sloped linearly away from a straight shoreline, domination by tidal currents favoured a convex hypsometry and domination by wind waves favoured a concave hypsometry.

Wood and Widdows (in press) have modelled the impact of biota on sediment erosion and deposition processes within muddy intertidal zones. Their depth averaged, 1-D model was aligned across the intertidal mudflat from the low water (LW) to HW locations [Figure 10(a)] and assumed that along-shore conditions were uniform. It was applied to intertidal transects located near the mouth of the Humber Estuary, U.K. The densities of Macoma balthica (a bioturbating small clam) and microphytobenthos (which produce sediment-stabilizing biopolymers) were specified along each transect [Figure 10(a)]. A sediment conservation equation was solved in order to investigate the effects of biota on sediment transport. The sediment erosion threshold was taken to be a linear function of diatom density, based on observations in the Westerschelde, Netherlands. Sediment erosion rate was calculated as a function of current speed and Macoma density, based on field and laboratory flume experiments that utilized varying Macoma numbers. They found that seasonal variation in the density of stabilizing microphytobenthos could alter net sediment deposition over a mudflat by a factor of two and inter-annual variation in the density of bioturbating clams by a factor of five.

Dynamic morphological models that attempt to simulate whole systems are much more complex, mathematically nonlinear and sensitive to perturbations in the initial and boundary conditions (Nicholson *et al.*, 1997). On the other hand, theoretical studies of sandy systems using simplified analytical concepts clearly demonstrate important features such as the dominant role of tidal currents and their flood-ebb asymmetry in shaping tidal basins (Dronkers, 1998; van de Kreeke, 1998). There have

been some theoretical studies on the morphodynamic stability of sandy tidal embayments that utilize more mechanistic dynamics (Mason & Garg, 2001; van Leeuwen and de Swart, 2001; Schuttelaaras & de Swart, 2000; van Leeuwen *et al.*, 2000). Although these ignore freshwater inputs and buoyancy effects, the studies provide insights into the role of tidal flows in morphological evolution. The main results are that the tidal and morphologic properties strongly depend on the sediment deposition process and on the length of the embayment. A depth-dependent deposition term caused bed profiles to become convex upwards, although with increasing length of embayment the bed profiles become concave. For funnel-shaped sandy estuaries, Lanzoni and Seminara (2002) found that two features characterized their modelled equilibrium bed profile: (i), a concavity that increased as the estuary convergence increased and (ii), a uniquely defined depth at the mouth.

The EMPHASYS project (EMPHASYS, 2000) has compared available morphological concepts and models with data from several estuaries, particularly the Humber and Mersey, U.K. The models were separated into three categories: top-down, bottom-up and hybrid. Top-down models can take two approaches: regime models and the expert analysis of data including the determination of trends and their extrapolation for prediction. The regime approach develops empirical relationships between dimensional measures of estuarine features, such as cross-sectional area, and their relationship to hydrodynamic variables such as tidal flow (e.g. Dennis *et al.*, 2000). Bottom-up methods rely on solving the dynamic equations for water and sediment transport, using calibration and validation data derived from short-term measurements. Hybrid models are a combination of top-down and bottom-up models (e.g. ESTMORF, Wang *et al.*, 1998). The bottom-up models are used to generate tidal elevations and current velocities for various bathymetric scenarios, and the regime theories are then used to test how close or how far the system may be from equilibrium.

A conclusion from EMPHASYS was that no individual model or approach could provide an adequate hindcast of the recorded morphological evolution of the chosen estuaries. Part of the reason for this may have been the poor resolution and accuracy of the available data and part due to the fact that no single model represented all of the relevant processes, especially those involving biology or waves. However, even for sandy systems where biological processes are likely to be less important, there are substantial differences between observed and predicted patterns of sediment movement (Mason & Garg, 2001).

## Summary

Recent modelling work and high-resolution measurements have shown that tidal straining of the longitudinal salinity field within partially mixed estuaries can result in nearly mixed or stratified conditions depending on the strength of tidal currents. Lower stratification (or complete mixing) tends to occur during strong spring tidal currents and significant stability during weaker currents. In general, maximum and minimum near-bed stratification occur during late ebb and flood, respectively, reflecting the dominant role played by tidal straining in determining intratidal variations in salinity and other key physical variables. It is a tribute to Pritchard's contribution to the field that 50 years after his work on estuarine circulation, researchers are still debating the precise nature of that circulation and its relationship to tidal straining (Stacey *et al.*, 2001). The same anniversary has also seen the deployment of instrumentation, far more sophisticated than was available to Pritchard, in field studies that essentially confirm his view of the role of vertical mixing in estuarine hydrodynamics and salt transport (Peters & Bokhurst, 2001).

The effects of waves and fine sediment suspensions on water column stability in turbid estuaries have been increasingly explored, especially through the use of numerical models. In very shallow areas, such as over intertidal mudflats, even small breaking waves appear to be capable of enhancing local turbidity. Although models demonstrate the damping of turbulence that is associated with high concentration, fine sediment suspensions, there appears to be no work that delineates the way in which this damping, or other consequences of suspended sediment transport, may potentially affect the large-scale hydrodynamic circulation or salt intrusion in estuaries.

The focus of recent work on strongly stratified estuaries has been on intratidal variations in stratification, as reflected in the depth and thickness of the pycnocline. These variations depend on the turbulent mixing generated by near-bed shear and that resulting from shear instabilities within the pycnocline, both of which are becoming more amenable to field observation and modelling. Measurements in the coastal zone and estuaries have determined turbulent energy dissipation throughout the water column at mixed and stratified sites and vertical profiles of Reynolds stress have been directly measured using ADCPs. These data show that energetic turbulence is confined to the bottom mixed layer by any overlying stratification and that the water column can be divided into regions based on the relative importance of buoyancy effects. The considerable progress that has been achieved with

turbulence modelling in recent years has been facilitated, partly, by the sharing of models and by collaborative projects such as the EU programme CARTUM (comparative analysis and rationalization of second-moment turbulence models).

Towed ADCPs have greatly increased our insight into transverse behaviour within estuaries and have essentially replaced labour-intensive, multi-station sampling of velocity. Strong transverse shears, convergence zones and non-linear features have been observed where bathymetric changes are sharpest, and increased stratification and decreased friction over channels, relative to the shoals, have been shown to modify tidal and residual flows. Detailed maps of surface tidal velocities and wind-driven and other currents have been derived from HF radar, although at scales that are currently only appropriate for coastal areas or larger estuaries. Satellite and airborne remote sensing now provides a unique view of spatial variability, especially frontal phenomena, and has demonstrated the importance of wave-induced suspension of fine sediments in shallow areas. Despite the sophistication of modern instruments, the complexity of transverse variability still prevents our attempts to accurately quantify, experimentally, the transport of SPM and solutes from estuaries to the coastal zone.

Transverse spatial variations in the ETM and their relationship to hydrodynamic frontal systems are being explored, along with the relationship between fine sediment characteristics and ETM formation. Parameterizations most likely to affect SPM models are those for particle aggregation, settling velocity and stratification-induced damping of vertical mixing. Aggregation is likely to be affected by ' sticky ' polymers produced by a wide range of organisms, including bacteria, invertebrates and especially benthic diatoms that inhabit the upper $10^{-3}$ m or so of intertidal mudflats. In stratified estuaries the fortnightly variation in SPM, characterized by low concentrations during neap tides and higher concentrations during springs, appears to result from a residual, up-estuary transport of near-bed sediment and its accumulation during the neap tide. In estuaries that are partly mixed and well mixed, a wide range of processes involving estuarine circulation, current shear, stratification and various tidal pumping mechanisms have been identified as important to the hydrodynamics of localized fine sediment accumulation. Sediment properties such as cohesion, erosion rates and thresholds, particle aggregation and settling velocity are equally important.

The EMPHASYS (2000) project led to several recommendations for future estuarine processes research that will be valuable in the context of sediment transport and morphology. One was to improve the prediction of wave generation, propagation and dissipation in estuaries in order to make allowance for shallow waters and short fetch lengths that vary temporally due to tidal covering and uncovering of tidal flats. Other recommendations were to improve the prediction of extreme wave and water levels within estuaries and to examine the effects of complex morphology on tidal processes, especially over the higher intertidal areas. Further requirements that were highlighted include the need to improve the representation of near-bed shear stresses in the presence of fluid mud and to understand better the transport of mixtures of sediments.

Despite the importance of morphological prediction, very little research has been carried out into medium space and time-scales and there have been relatively few interdisciplinary studies to examine the relationships between biology and morphology. What measurements have been made to correlate measured erosion properties and biological characteristics of intertidal mudflats show that bivalve activity and the surface diatom biofilm can be important in controlling the initial erosion of the surface mud layer. Studies have demonstrated that biota can alter sediment erosion rates by more than two orders of magnitude. Spatial variability in rates is largely dependent on the changes in biota and sediment properties that occur with shore height. Temporal variability is both seasonal and inter-annual. Seasonal growth patterns of benthic microalgae, macroalgal mats and salt marsh plants have a marked effect, although inter-annual variation tends to be greater. This results primarily from the impact of climatic events and cycles on the distribution and abundance of key biota. As a geographically dependent example, rates of sediment erosion on an intertidal mudflat may increase in the year after a cold winter due to possible increases in the abundance of the bioturbating clam, Macoma, which in turn may lead to increased accretion on adjacent salt marshes.

Perhaps one of the most intriguing results of recent estuarine process research has been this increased awareness of biological-physical interactions. The incorporation of biological processes into sediment transport and morphological models would seem to be an important step in future attempts to forecast changes in sediment erosion, transport and deposition in response to the different scenarios that are likely to result from climate change and sea level rise. In all of these efforts to improve our understanding of water column, sediment and morphological physical processes, numerical and analytical models of varying complexity (e.g. spatial dimension and sophistication

of turbulence closure scheme) have been and will continue to be essential to the insights gained.

## Acknowledgements

I am grateful to Professor K. R. Dyer, Dr A. J. Bale and Dr J. Widdows for discussions on estuarine morphology, particle aggregation (including EPS), and bio-sediment interactions, respectively. I thank Dr R. Lewis and Mr J. Lewis of Astrazeneca's Brixham Environmental Laboratory, U.K., for their fieldwork collaboration in obtaining the data shown in Figure 5, and Mrs C. Harris for her assistance with the collation of reprints for the preparation of this article.

## References

Alvarez, O., Izquierdo, A., Tejedor, B., Mañanes, R., Tejedor, L. & Kagan, B. A. 1999 The influence of sediment load on tidal dynamics, a case study: Cadiz Bay. *Estuarine, Coastal and Shelf Science* **48,** 439–450.

Amos, C. L., Feeney, T., Sutherland, T. F. & Luternauer, J. L. 1997 The stability of fine-grained sediments from the Fraser River delta. *Estuarine, Coastal and Shelf Science* **45,** 507–524.

Anderson, T. J. 2001 Seasonal variation in erodibility of two temperate, microtidal mudflats. *Estuarine, Coastal and Shelf Science* **53,** 1–12.

Bale, A. J., Uncles, R. J., Widdows, J., Brinsley, M. & Barrett, C. D. (in press) Direct observation of the formation and break-up of aggregates in an annular flume using laser reflectance particle sizing. In *Proceedings of the INTERCOH conference*, Delft Hydraulics, Sept 4–8, 2000.

Blanton, J. O., Amft, J. & Tisue, T. 1997 Response of a small-scale bottom-attached estuarine plume to wind and tidal dissipation. *Journal of Coastal Research* **13,** 349–362.

Boicourt, W.C. 1992 Influences of circulation processes on dissolved oxygen in Chesapeake Bay. In *Oxygen Dynamics in the Chesapeake Bay* (Smith, D. E., Leffler, M. & Mackiernan, G., eds). Pub. Maryland Sea Grant College, Maryland, USA, pp. 7–59.

Bowen, M. M. 1999 Mechanisms and variability of salt transport in partially-stratified estuaries. Thesis for the degree of Doctor of Philosophy at the Massachusetts Institute of Technology and the Woods Hole Oceanographic Institute, September 1999, 171 pp.

Brown, J., Turrell, W. R. & Simpson, J. H. 1991 Aerial surveys of axial convergence fronts in UK estuaries and the implications for pollution. *Marine Pollution Bulletin* **22,** 397–400.

Brubaker, J. M. & Simpson, J. H. 1999 Flow convergence and stability at a tidal estuarine front: Acoustic Doppler current observations. *Journal of Geophysical Research* **104** (C8), 18257–18268.

Burchard, H. 2001*a* Simulating the wave-enhanced layer under breaking surface waves with two-equation turbulence models. *Journal of Physical Oceanography* **31,** 3133–3145.

Burchard, H. 2001*b* On the $q^2l$ equation by Mellor and Yamada (1982). *Journal of Physical Oceanography* **31,** 1377–1387.

Burchard, H. & Bolding, K. 2001 Comparative analysis of four second-moment turbulence closure models for the oceanic mixed layer. *Journal of Physical Oceanography* **31,** 1943–1968.

Burchard, H., Bolding, K. & Villarreal, M. R. 1999 GOTM—A General Ocean Turbulence Model. Theory, implementation and test cases. Joint Research Centre, European Commission, EUR 8745EN, 103 pp.

Burchard, H. & Baumert, H. 1998 The formation of estuarine turbidity maxima due to density effects in the salt wedge. A hydrodynamic process study. *Journal of Physical Oceanography* **28,** 309–321.

Burchard, H., Petersen, O. & Rippeth, T. P. 1998 Comparing the performance of the Mellor-Yamada and the $\kappa$–$\varepsilon$ two-equation turbulence models. *Journal of Geophysical Research* **103** (C5), 10543–10554.

Burrus, C. S., Gopinath, R. A. & Guo, H. 1998 *Introduction to Wavelets and Wavelet Transforms: a primer*. Prentice Hall, Upper Saddle River, New Jersey, 268 pp.

Chant, R. J. & Stoner, A. W. 2001 Particle trapping in a stratified flood-dominated estuary. *Journal of Marine Research* **59,** 29–51.

Cheng, R. T., Ling, C.-H., Gartner, J. W. & Wang, P. F. 1999 Estimates of bottom roughness length and bottom shear stress in South San Francisco Bay, California. *Journal of Geophysical Research* **104** (C4), 7715–7728.

Cheng, R. T., Casulli, V. & Gartner, J. W. 1993 Tidal, Residual, Intertidal Mudflat (TRIM) model and its applications to San Francisco Bay, California. *Estuarine, Coastal and Shelf Science* **36,** 235–280.

Christie, M. C., Dyer, K. R. & Turner, P. 1999 Sediment flux and bed level measurements from a macro tidal mudflat. *Estuarine, Coastal and Shelf Science* **49,** 667–688.

Cisneros-Aguirre, J., Pelegrí, J. L. & Sangrà, P. 2001 Experiments on layer formation in stratified shear flow. *Scientia Marina* **65,** 117–126.

Collins, M. B., Ke, X. & Gao, S. 1998 Tidally-induced flow structure over intertidal flats. *Estuarine, Coastal and Shelf Science* **46,** 233–250.

Cudaback, C. N. & Jay, D. A. 2001 Tidal asymmetry in an estuarine pycnocline 2: Transport. *Journal of Geophysical Research* **106** (C2), 2639–2652.

Cudaback, C. N. & Jay, D. A. 2000 Tidal asymmetry in an estuarine pycnocline: depth and thickness. *Journal of Geophysical Research* **105** (C11), 26237–26251.

Davies, A. M., Hall, P., Howarth, M. J., Knight, P. J. & Player, R. J. 2001 Comparison of observed (HF radar and ADCP measurements) and computed tides in the North Channel of the Irish Sea. *Journal of Physical Oceanography* **31,** 1764–1785.

Dearnaley, M. P. 1997 Direct measurements of settling velocities in the Owen Tube: a comparison with gravimetric analysis. In *Cohesive sediments* (Burt, N., Parker, R. & Watts, J., eds). John Wiley, Chichester, 458 pp.

Dennis, J. M., Spearman, J. R. & Dearnaley, M. P. 2000 The development of regime models for prediction of the long-term effects of civil engineering activities on estuaries. *Journal of Physics and Chemistry of the Earth (B)* **25,** 45–50.

Dronkers, J. 1998 Morphodynamics of the Dutch Delta. In *Physics of Estuaries and Coastal Seas* (Dronkers, J. & Scheffers, M. B. A. M., eds). Balkema, Rotterdam, pp. 297–304.

Dyke, P. P. G. 2001 *Coastal and Shelf Sea Modelling. Kluwer International Series: Topics in Environmental Fluid Mechanics*. Kluwer Academic Publisher, London, 257 pp.

Dyer, K. R. 2000 Preface to the special issue on intertidal mudflats. In *Nearshore and Coastal Oceanography* (Huntley, D. A. & Oltman-Shay, O., eds). *Continental Research* **20** (10–13), 1037–1038.

Dyer, K. R., Christie, M. C. & Wright, E. W. 2000 The classification of intertidal mudflats. In *Nearshore and Coastal Oceanography* (Huntley, D. A. & Oltman-Shay, O., eds). *Continental Research* **20** (10–13), 1039–1060.

Dyer, K. R. & Manning, A. J. 1999 Observation of the size, settling velocity and effective density of flocs, and their fractal dimensions. *Journal of Sea Research* **41,** 87–95.

Dyer, K. R. 1997 *Estuaries: a Physical Introduction*. John Wiley, Chichester, 195 pp.

Dyer, K. R. 1986 *Estuarine and Coastal Sediment Dynamics*. John Wiley, Chichester, 342 pp.

EMPHASYS 2000 Modelling estuary morphology and process. Final Report of the Emphasys Consortium, Report TR 111, Hydraulics Research, Wallingford, Oxon, UK. 193 pp.

ERF15 2001 Processes and products of the estuarine turbidity maximum (symposium papers from the 15th biennial Estuarine Research Federation conference). *Estuaries* **24,** 655–786.

Fain, A. M. V., Jay, D. A., Wilson, D. J., Orton, P. M. & Baptista, A. M. (in press) Seasonal and tidal-monthly patterns of particulate matter dynamics in a river estuary. *Estuaries*.

Farmer, D. M. & Armi, L. 1986 Maximal two-layer exchange over a sill and through the combination of a sill and contraction with net barotropic flow. *Journal of Fluid Mechanics* **164,** 53–76.

Ferrier, G. & Anderson, J. M. 1997*a* A multidisciplinary study of frontal systems in the Tay Estuary, Scotland. *Estuarine, Coastal and Shelf Science* **45,** 317–336.

Ferrier, G. & Anderson, J. M. 1997*b* The application of remotely sensed data in the study of frontal systems in the Tay Estuary. *International Journal of Remote Sensing* **18,** 2035–2065.

Fischer, H. B. 1972 Mass transport mechanisms in partially stratified estuaries. *Journal of Fluid Mechanics* **53,** 671–687.

Flinchem, E. P. & Jay, D. A. 2000 An introduction to wavelet transform tidal analysis methods. *Estuarine, Coastal and Shelf Science* **51,** 177–200.

Friedrichs, C. T., Armbrust, B. D. & de Swart, H. E. 1998 Hydrodynamics and equilibrium sediment dynamics of shallow, funnel-shaped tidal estuaries. In *Physics of Estuaries and Coastal Seas* (Dronkers, J. & Scheffers, M. B. A. M.). Balkema, Rotterdam, pp. 315–327.

Friedrichs, C.T. & Wright, L. D. 1997 Sensitivity of bottom stress and bottom roughness estimates to density stratification, Eckernförde Bay, southern Baltic Sea. *Journal of Geophysical Research* **102** (C3), 5721–5732.

Friedrichs, C. T. & Hamrick, J. M. 1996 Effects of channel geometry on cross sectional variations in along channel velocity in partially stratified estuaries. In *Buoyancy Effects on Coastal and Estuarine Dynamics* (Aubrey, D. G. & Friedrichs, C. T., eds). *American Geophysical Union* **53,** 283–300.

Friedrichs, C. T. & Aubrey, D. O. 1996 Uniform bottom shear stress and equilibrium hypsometry of intertidal flats. In *Mixing in Estuaries and Coastal Seas* (Pattiaratchi, C., ed.). Coastal and Estuarine Studies 50, *American Geophysical Union*, 405–429.

Gartner, J. W., Cheng, R., Wang, P.-F. & Richter, K. 2001 Laboratory and field evaluations of the LISST-100 instrument for suspended particle size determinations. *Marine Geology* **175,** 199–219.

Gilcoto, M., Álvarez-Salgado, X. A. & Pérez, F. F. 2001 Computing optimum estuarine residual fluxes with a multiparameter inverse method (OERFIM): application to the Ria de Vigo (NW Spain). *Journal of Geophysical Research* **106** (C12), 31303–31318.

Geyer, W. R., Woodruff, J. D. & Traykovski, P. 2001 Sediment transport and trapping in the Hudson River Estuary. *Estuaries* **24,** 670–679.

Geyer, W. R., Trowbridge, J. H. & Bowen, M. M. 2000 The dynamics of a partially mixed estuary. *Journal of Physical Oceanography* **30,** 2035–2048.

Geyer, W. R., Signell, R. P. & Kineke, G. C. 1998 Lateral trapping of sediment in a partially mixed estuary. In *Physics of Estuaries and Coastal Seas* (Dronkers, J. & Scheffers, M. B. A. M., eds). Balkema, Rotterdam, pp. 115–126.

Geyer, W. R. 1997 Influence of wind on dynamics and flushing of shallow estuaries. *Estuarine, Coastal and Shelf Science* **44,** 713–722.

Geyer, W. R. & Nepf, H. 1996 Tidal pumping of salt in a moderately stratified estuary. In *Buoyancy Effects on Coastal and Estuarine Dynamics* (Aubrey, D. G. & Friedrich, C. T., eds). Coastal and Estuarine Studies 53, *American Geophysical Union*, 213–226.

Goodberlet, M. A., Swift, C. T., Kiley, K. P., Miller, J. L. & Zaitzeff, J. B. 1997 Microwave remote sensing of coastal zone salinity. *Journal of Coastal Research* **13,** 363–372.

Grabemann, I. & Krause, G. 2001 On different time scales of suspended matter dynamics in the Weser Estuary. *Estuaries* **24,** 688–698.

Green, M. O. & MacDonald, I. T. 2001 Processes driving estuary infilling by marine sands on an embayed coast. *Marine Geology* **178,** 11–37.

Green, M. O., Black, K. P. & Amos, C. L. 1997 Control of estuarine sediment dynamics by interactions between currents and waves at several scales. *Marine Geology* **144,** 97–116.

Guézennec, L., Lafite, R., Dupont, J.-P., Meyer, R. & Boust, D. 1999 Hydrodynamics of suspended particulate matter in the tidal freshwater zone of a macrotidal estuary (the Seine Estuary, France). *Estuaries* **22,** 717–727.

Hansen, D. V. & Rattray, M. Jr. 1965 Gravitational circulation in straits and estuaries. *Journal of Marine Research* **23,** 104–122.

Helfrich, K. 1995 Time-dependent two-layer hydraulic exchange flows. *Journal of Physical Oceanography* **25,** 359–373.

Hearn, C. J. 1998 Application of the Stommel model to shallow Mediterranean estuaries and their characterization. *Journal of Geophysical Research* **103,** 10391–10404.

Hill, P. S., Milligan, T. G. & Geyer, W. R. 2000 Controls on effective settling velocity of suspended sediment in the Eel River flood plume. *Continental Shelf Research* **20,** 2095–2111.

Holt, J. T. & James, I. D. 2001 An s-coordinate density evolving model of the northwest European continental shelf. Part 1: Model description and density structure. *Journal of Geophysical Research* **106** (C7), 14015–14034.

Huang, W. & Foo, S. 2002 Neural network modelling of salinity variation in Apalachicola River. *Water Research* **36,** 356–362.

Huzzey, L. M. & Brubaker, J. M. 1988 The formation of longitudinal fronts in a coastal plain estuary. *Journal of Geophysical Research* **93,** 1329–1334.

IPCC 2001 Climate Change: The Scientific Basis. Contribution of Working Group I to the third assessment report of the intergovernmental panel on climate change (IPCC). (Houghton, J. T., Ding, Y., Griggs, D. J., Noguer, M., van der Linden, P. J. & Xiaosu, D., eds). Cambridge University Press, UK, 944 pp.

Jay, D. A. & Flinchem, E. P. 1997 Interaction of fluctuating river flow with a barotropic tide: a demonstration of wavelet tidal analysis methods. *Journal of Geophysical Research* **102** (C3), 5705–5720.

Joordens, J. C. A., Souza, A. J. & Visser, A. 2001 The influence of tidal straining and wind on suspended matter and phytoplankton distribution in the Rhine outflow region. *Continental Shelf Research* **21,** 301–325.

Kappenberg, J. & Grabemann, I. 2001 Variability of the mixing zones and estuarine turbidity maxima in the Elbe and Weser Estuaries. *Estuaries* **24,** 688–698.

Kay, D. J. & Jay, D. A. (in press) (*a*) Interfacial mixing in a highly-stratified estuary. 1: Characteristics of mixing. *Journal of Geophysical Research*.

Kay, D. J. & Jay, D. A. (in press) (*b*) Interfacial mixing in a highly-stratified estuary. 2: A ' method of constrained differences ' approach for the determination of the momentum and mass balances and the energy of mixing. *Journal of Geophysical Research*.

Kjerfve, B. & Proehl, J. A. 1979 Velocity variability in a cross-section of a well-mixed estuary. *Journal of Marine Research* **37,** 409–418.

Kocsis, O., Prandke, H., Stips, A., Simon, A. & Wüest, A. 1999 Comparison of dissipation of turbulent kinetic energy determined from shear and temperature microstructure. *Journal of Marine Systems* **21,** 67–84.

Krone, R. B. 1993 Sedimentation revisited. In *Nearshore and Estuarine Cohesive Sediment Transport* (Mehta, A. J., ed.). Coastal and Estuarine Studies **42,** AGU, Washington, pp. 108–125.

Lacy, J. R. & Monismith, S. G. 2001 Secondary currents in a curved, stratified, estuarine channel. *Journal of Geophysical Research* **106** (C12), 31238–31302.

Lane, A., Prandle, D., Harrison, A. J., Jones, P. D. & Jarvis, C. J. 1997 Measuring fluxes in tidal estuaries: sensitivity to

instrumentation and associated data analyses. *Estuarine, Coastal and Shelf Science* **45,** 433–451.
Lanzoni, S. & Seminara, G. 2002 Long-term evolution and morphodynamic equilibrium of tidal channels. *Journal of Geophysical Research* **107** (C1), 1–13.
Largier, J. L. 1992 Tidal intrusion fronts. *Estuaries* **15,** 26–39.
Law, D. J., Bale, A. J. & Jones, S. E. 1997 Adaptation of focused beam reflectance measurement to in-situ particle sizing in estuaries and coastal waters. *Marine Geology* **140,** 47–59.
Lawler, D. M., West, J. R., Couperthwaite, J. S. & Mitchell, S. B. 2001 Application of a novel automatic erosion and deposition monitoring system at a channel bank site on the tidal River Trent, UK. *Estuarine, Coastal and Shelf Science* **53,** 237–247.
Le Hir, P., Fight, A., Jacinto, R. S., Lesueur, P., Dupont, J.-P., Lafite, R., Brenon, I., Thouvenin, B. & Cugier, P. 2001 Fine sediment transport and accumulations at the mouth of the Seine Estuary (France). *Estuaries* **24,** 950–963.
Leatherman, S. P. 2001 Social and economic costs of sea level rise. In *Sea Level Rise: history and consequences* (Douglas, B. C., Kearney, M. S. & Leatherman, S. P., eds). International Geophysics Series 75. Academic Press, San Diego, pp. 181–223.
Lewis, R. 1997 *Dispersion in Estuaries and Coastal Waters*. John Wiley, Chichester, 312 pp.
Li, C. & O'Donnell, J. 1997 Tidally driven residual circulation in shallow estuaries with lateral depth variation. *Journal of Geophysical Research* **102** (C13), 27915–27929.
Li, C. & Valle-Levinson, A. 1999 A two-dimensional analytic tidal model for a narrow estuary of arbitrary lateral depth variation: the intratidal motion. *Journal of Geophysical Research* **104** (C10), 23525–23543.
Lick, W., Huang, H. & Jepson, R. 1993 Flocculation of fine-grained sediments due to differential settling. *Journal of Geophysical Research* **98** (C6), 10279–10288.
Luyten, P. J. E., Deleersnijder, E., Ozer, J. & Ruddick, K. G. 1996 Presentation of a family of turbulence closure models of stratified shallow water flows and application to the Rhine outflow region. *Continental Shelf Research* **16,** 101–130.
Madsen, J. D., Chambers, P. A., James, W. F., Koch, E. W. & Westlake, D. F. 2001 The interaction between water movement, sediment dynamics and submerged macrophytes. *Hydrobiologia* **444,** 71–84.
Manning, A. J. & Dyer, K. R. 1999 A laboratory examination of floc characteristics with regard to turbulent shearing. *Marine Geology* **160,** 147–170.
Marmorino, G. O. & Trump, C. L. 2000 Gravity current structure of the Chesapeake Bay outflow plume. *Journal of Geophysical Research* **105** (C12), 28847–28861.
Mason, D. C. & Garg, P. K. 2001 Morphodynamic modelling of intertidal sediment in Morcombe Bay. *Estuarine, Coastal and Shelf Science* **53,** 79–92.
McAnally, W. H. & Mehta, A. J. 2001 *Coastal and Estuarine Fine Sediment Processes*. Elsevier Science, Amsterdam, 540 pp.
McManus, J. 1998 Temporal and spatial variations in estuarine sedimentation. *Estuaries* **21,** 622–634.
Mehta, A. J. 1993 *Nearshore and Estuarine Cohesive Sediment Transport*. Coastal and Estuarine Studies **42.** AGU, Washington, 581 pp.
Mei, C. C., Fan, S. & Jin, K. 1997 Resuspension and transport of fine sediments by waves. *Journal of Geophysical Research* **102** (C7), 15807–15821.
Mocke, G. P. 2001 Structure and modelling of surf zone turbulence due to wave breaking. *Journal of Geophysical Research* **106** (C8), 17039–17057.
Möller, I., Spencer, T., French, J. R., Leggett, D. J. & Dixon, M. 1999 Wave transformation over salt marshes: a field and numerical modelling study from North Norfolk, England. *Estuarine, Coastal and Shelf Science* **49,** 411–426.
Monismith, S. G. & Fong, D. A. 1996 A simple model of mixing in stratified tidal flows. *Journal of Geophysical Research* **101** (C12), 28583–28595.
Nepf, H. M. & Geyer, W. R. 1996 Intratidal variations in stratification and mixing in the Hudson estuary. *Journal of Geophysical Research* **101** (C5), 12079–12086.
Nicholson, J., Broker, I., Roelvink, J. A., Price, D., Tanguy, J. M. & Moreno, L. 1997 Intercomparison of coastal area morphodynamic models. *Coastal Engineering* **31,** 97–123.
Nimmo Smith, W. A. M. & Thorpe, S. A. 1999 Dispersion of buoyant material by Langmuir circulation and a tidal current. *Marine Pollution Bulletin* **38,** 824–829.
O'Donnell, J., Marmorino, G. O. & Trump, C. L. 1998 Convergence and downwelling at a river plume front. *Journal of Physical Oceanography* **28,** 1481–1495.
Officer, C. B. 1976 *Physical Oceanography of Estuaries (and associated coastal waters)*. John Wiley, New York, 465 pp.
Orton, P. M. & Kineke, G. C. 2001 Comparing calculated and observed vertical suspended-sediment distributions from a Hudson River estuary turbidity maximum. *Estuarine, Coastal and Shelf Science* **52,** 401–410.
Orton, P. M., Wilson, D. J., Jay, D. A. & Fain, A. M. V. (in press) High resolution sediment dynamics in salt-wedge estuaries. In *Southwest Washington Coastal Erosion Workshop Report 2000* (Gelfenbaum, G. & Kaminsky, G., eds). US Geological Survey.
Paterson, D. M., Tolhurst, T. J., Kelly, J. A., Honeywill, C., de Deckere, E. M. G. T., Huet, V., Shayler, S. A., Black, K. S., de Brouwer, J. & Davidson, I. 2000 Variations in sediment properties, Skeffling mudflat, Humber Estuary, UK. *Continental Shelf Research* **20,** 1373–1396.
Pattiaratchi, C., Hegge, B., Gould, J. & Eliot, I. 1997 Impact of sea-breeze activity on nearshore and foreshore processes in southwestern Australia. *Continental Shelf Research* **17,** 1539–1560.
Pattiaratchi, C., Lavery, P., Wyllie, A. & Hick, P. 1994 Estimates of water quality in coastal waters using multi-date Landsat Thematic Mapper data. *International Journal of Remote Sensing* **15,** 1571–1584.
Peters, H. & Bokhorst, R. 2001 Microstructure observations of turbulent mixing in a partially mixed estuary, Part II: salt flux and stress. *Journal of Physical Oceanography* **31,** 1105–1119.
Peters, H. 1999 Spatial and temporal variability of turbulent mixing in an estuary. *Journal of Marine Research* **57,** 805–845.
Peters, H. 1997 Observations of stratified turbulent mixing in an estuary: neap-to-spring variations during high river flow. *Estuarine, Coastal and Shelf Science* **45,** 69–88.
Postma, H. 1967 Sediment transport and sedimentation in the estuarine environment. In *Estuaries* (Lauff G. H., ed.). Wiley, New York, pp. 158–179.
Prandle, D. 1997*a* Tidal and wind-driven currents from OSCR. *Oceanography* **10,** 57–59.
Prandle, D. 1997*b* Tidal characteristics of suspended sediment concentrations. *Journal of Hydraulic Engineering* **123,** 341–350.
Prandle, D. & Ryder, K. D. 1985 Measurement of surface currents in Liverpool Bay by high frequency radar. *Nature* **315,** 128–131.
Pratt, L. J. 1986 Hydraulic control of sill flow with bottom friction. *Journal of Physical Oceanography* **16,** 1970–1980.
Pritchard, D. W. 1956 The dynamic structure of a coastal plain estuary. *Journal of Marine Research* **15,** 33–42.
Pritchard, D. W. 1954 A study of the salt balance in a coastal plain estuary. *Journal of Marine Research* **13,** 133–144.
Pritchard, D. W. 1952 Salinity distribution and circulation in the Chesapeake Bay estuarine system. *Journal of Marine Research* **11,** 106–123.
Riethmüller, R., Heineke, M., Kühl, H. & Keuker-Rüdiger, R. 2000 Chlorophyll a concentration as an index of sediment surface stabilization by microphytobenthos? In *Nearshore and Coastal Oceanography* (Huntley, D. A. & Oltman-Shay, O., eds). *Continental Research* **20** (10–13), 1351–1372.
Rippeth, T., Fisher, N. & Simpson, J. H. 2001 The cycle of turbulent dissipation in the presence of tidal straining. *Journal of Physical Oceanography* **31,** 2458–2471.
Ris, R. C., Booij, N. & Holthuijsen, L. H. 1999 A third-generation wave model for coastal regions, Part II: verification. *Journal of Geophysical Research* **104** (C4), 7667–7681.

Ruhl, C. A., Schoellhamer, D. H., Stumpf, R. P. & Lindsay, C. L. 2001 Combined use of remote sensing and continuous monitoring to analyze the variability of suspended-sediment concentrations in San Francisco Bay, California. *Estuarine, Coastal and Shelf Science* **53,** 801–812.

Sanford, T. B., Suttles, S. E. & Halka, J. P. 2001 Reconsidering the physics of the Chesapeake Bay estuarine turbidity maximum. *Estuaries* **24,** 655–669.

Sanford, T. B. & Lien, R.-C. 1999 Turbulent properties in a homogeneous bottom tidal boundary layer. *Journal of Geophysical Research* **104** (C1), 1245–1257.

Schuttelaaras, H. M. & de Swart, H. E. 2000 Multiple morphodynamic equilibria in tidal embayments. *Journal of Geophysical Research* **105** (C10), 24105–24118.

Shaowu, L., Shangyi, W. & Shibayama, T. 1998 A nearshore wave breaking model. *Acta Oceanologica Sinica* **17,** 133–139.

Sharp1es, J., Simpson, J. H. & Brubaker, J. M. 1994 Observations and modelling of periodic stratification in the Upper York River Estuary, Virginia. *Estuarine, Coastal and Shelf Science* **38,** 301–312.

Shen, C. Y. & Evans, T. E. 2001 Surface-to-surface velocity projection for shallow water currents. *Journal of Geophysical Research* **106** (C4), 6973–6984.

Siddorn, J. R., Allen, J. I. & Uncles, R. J.(in press) Heat, salt and tracer transport in the Plymouth Sound coastal region: a 3D modelling study. *Journal of the Marine Biological Association of the UK.*

Simpson, J. H., Vennell, R. & Souza, A. J. 2001 The salt fluxes in a tidally-energetic estuary. *Estuarine, Coastal and Shelf Science* **52,** 131–142.

Simpson, J. H., Crawford, W. R., Rippeth, T. P., Campbell, A. R. & Cheok, J. V. S. 1996 The vertical structure of turbulent dissipation in shelf seas. *Journal of Physical Oceanography* **26,** 1579–1590.

Simpson, J. H. & Souza, A. J. 1995 Semidiurnal switching of stratification in the region of freshwater influence of the Rhine. *Journal of Geophysical Research* **100** (C4), 7037–7044.

Smith, R. & Scott, C. F. 1997 Mixing in the tidal environment. *Journal of Hydraulic Engineering* **123,** 332–340.

Stacey, M. T., Burau, J. R. & Monismith, S. G. 2001 Creation of residual flows in a partially stratified estuary. *Journal of Geophysical Research* **106** (C8), 17013–17037.

Stacey, M. T., Monismith, S. G. & Burau, J. R. 1999 Observations of turbulence in a partially stratified estuary. *Journal of Physical Oceanography* **29,** 1950–1970.

Tolhurst, T. J., Black, K. S., Shayler, S. A., Mather, S., Black, I., Baker, K. & Paterson, D. M. 1999 Measuring the in-situ erosion shear stress of intertidal sediments with the cohesive strength meter (CSM). *Estuarine, Coastal and Shelf Science* **49,** 281–294.

Tolman, H. L. & Booij, N. 1998 Modeling wind waves using wavenumber-direction spectra and a variable wavenumber grid. *The Global Atmosphere and Ocean System* **6,** 295–309.

Townsend, A. A. 1956 *The Structure of Turbulent Shear Flow*. Cambridge monographs on mechanics and applied mathematics. Cambridge University Press, 315 pp.

Trowbridge, J. H., Geyer, W. R., Bowen, M. M. & Williams, A. J. 1999 Near-bottom turbulence measurements in a partially mixed estuary: turbulent energy balance, velocity structure, and along-channel momentum balance. *Journal of Physical Oceanography* **29,** 3056–3072.

Turner, J. S. 1973 *Buoyancy Effects in Fluids*. Cambridge Monographs on Mechanics and Applied Mathematics. Cambridge University Press, 368 pp.

Valle-Levinson, A., Delgado, J. A. & Atkinson, L. P. 2001 Reversing water exchange patterns at the entrance to a semiarid coastal lagoon. *Estuarine, Coastal and Shelf Science* **53,** 825–838.

Valle-Levinson, A., Wong, K.-C. & Lwiza, K. M. M. 2000*a* Fortnightly variability in the transverse dynamics of a coastal plain estuary. *Journal of Geophysical Research* **105** (C2), 3413–3424.

Valle-Levinson, A., Li, C., Wong, K.-C. & Lwiza, K. M. M. 2000*b* Convergence of lateral flow along a coastal plain estuary. *Journal of Geophysical Research* **105** (C7), 17045–17061.

Valle-Levinson, A. & Atkinson, L. P. 1999 Spatial gradients in the flow over an estuarine channel. *Estuaries* **22,** 179–193.

Valle-Levinson, A. & Wi1son, R. E. 1998 Rotation and vertical mixing effects on volume exchange in eastern Long Island Sound. *Estuarine, Coastal and Shelf Science* **46,** 573–585.

Valle-Levinson, A., Li, C., Royer, T. C. & Atkinson, L. P. 1998 Flow patterns at the Chesapeake Bay entrance. *Continental Shelf Research* **18,** 1157–1177.

Van de Kreeke, J. 1998 Adaptation of the Frisian Inlet to a reduction in basin area with special reference to the cross-sectional area of the inlet channel. In *Physics of Estuaries and Coastal Seas* (Dronkers, J. & Scheffers, M. B. A. M., eds). Balkema, Rotterdam, pp. 355–362.

Van Leeuwen, S. M. & de Swart, H. E. 2001 The effect of advective processes on the morphodynamic stability of short tidal embayments. *Journal of Physics and Chemistry of the Earth (B)* **26,** 735–740.

Van Leeuwen, S. M., Schuttelaars, H. M. & de Swart, H. E. 2000 Tidal and morphologic properties of embayments: effect of sediment deposition processes and length variation. *Journal of Physics and Chemistry of the Earth (B)* **25,** 365–368.

Van Leussen, W. 1999 The variability of settling velocities of suspended fine-grained sediment in the Ems Estuary. *Journal of Sea Research* **41,** 109–118.

Van Leussen, W. 1994 *Estuarine Macroflocs and their Role in Fine-grained Sediment Transport*. Cip-Gegevens Koninklijke Bibliotheek, Den Haag, The Netherlands, 484 pp.

Van Wijnen, H. J. & Bakker, J. P. 2001 Long-term surface elevation change in salt marshes: a prediction of marsh response to future sea level rise. *Estuarine, Coastal and Shelf Science* **52,** 381–390.

Walters, R. A. 1997 A model study of tidal and residual flow in Delaware Bay and River. *Journal of Geophysical Research* **102,** 12689–12704.

Wang, Z. B., Karssen, B., Fokkink, R. J. & Langerak, A. 1998 A dynamic-empirical model for estuarine morphology. In *Physics of Estuaries and Coastal Seas* (Dronkers, J. & Scheffers, M. B. A. M., eds). Balkema, Rotterdam, pp. 279–296.

Winterwerp, J. C. 2001 Stratification effects by cohesive and noncohesive sediment. *Journal of Geophysical Research* **106** (C10), 22559–22574.

Wood, R. & Widdows, J. (in press) A model of sediment transport over an intertidal transect, comparing the influences of biological and physical factors. *Limnology and Oceanography*.

Widdows, J. 2001 The intertidal zone. In *Land-ocean Interaction: measuring and modelling fluxes from river basins to coastal seas* (Huntley, D. A., Leeks, G. J. L. & Walling, D. E., eds). IWA Publishing, London, pp. 184–208.

Wolanski, E., Nguyen Ngoc Huan, Le Trong Dao, Nguyen Huu Nhan & Nguyen Ngoc Thuy 1996 Fine-sediment dynamics in the Mekong River Estuary, Vietnam. *Estuarine, Coastal and Shelf Science* **43,** 565–582.

Wong, K.-C. & Moses-Hall, J. E. 1998 The tidal and subtidal variations in the transverse salinity and current distributions across a coastal plain estuary. *Journal of Marine Research* **56,** 489–517.

Wright, L. D., Schaffner, L. C. & Maa, J. P.-Y. 1997 Biological mediation of bottom boundary layer processes and sediment suspension in the lower Chesapeake Bay. *Marine Geology* **141,** 27–50.

Zhou, M. 1998 Influence of bottom stress on the two-layer flow induced by gravity currents in estuaries. *Estuarine, Coastal and Shelf Science* **46,** 811–825.

## Appendix

**A1:** ‘ Tidal straining ’ of the salinity field refers to the displacement of isohalines by tidal (and usually

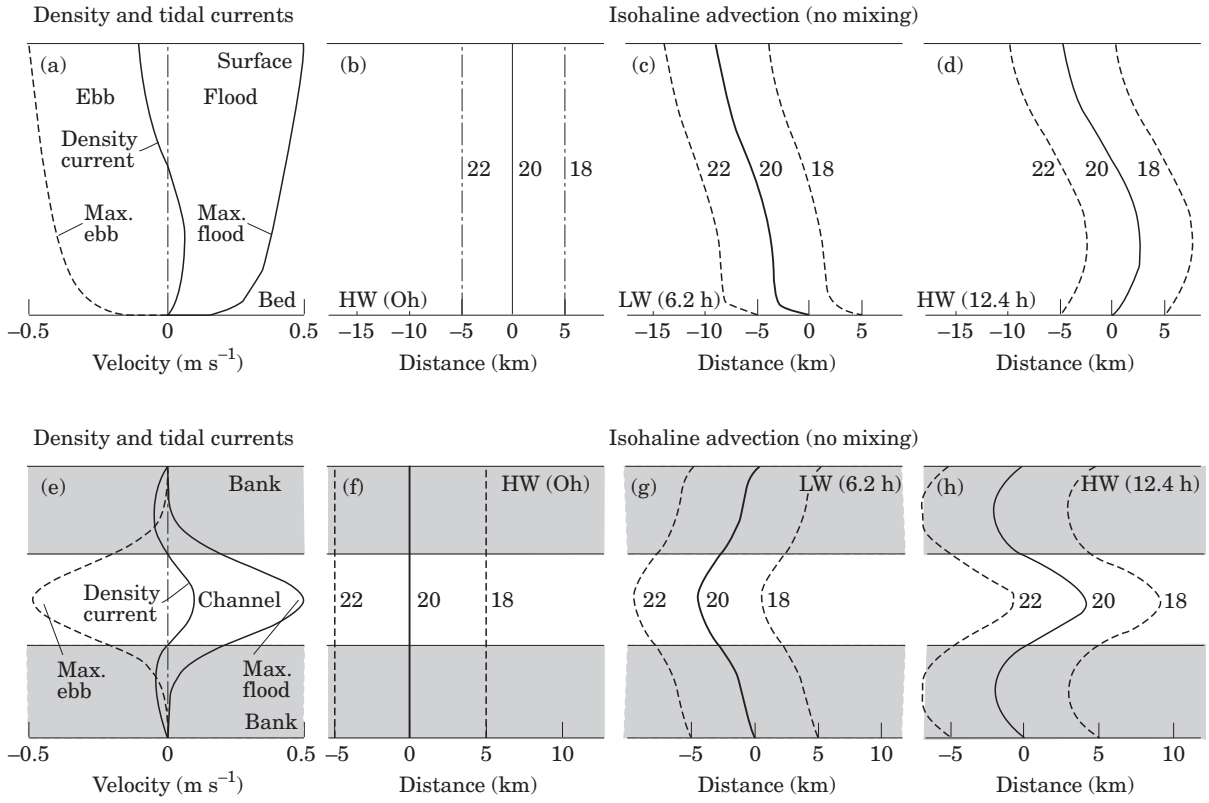


FIGURE A1. Schematic illustration of the effects of tidal current straining on the vertical, (a)–(d), and horizontal, (e)–(h), distributions of equally spaced 18–22 isohalines in a laterally uniform and vertically uniform estuary, respectively. Mixing and freshwater runoff are ignored, so that these examples would eventually generate 'run-away' vertical or lateral salinity gradients. The summation of tidal and density currents, shown separately on (a), produces enhanced flood currents in the lower water column and enhanced ebb currents in the upper water column. Starting at high water (HW) with uniformly spaced and vertically mixed 18–22 isohalines, (b), then in the absence of mixing, down-estuary advection on the ebb leads to salinity stratification at low water (LW), (c). Up-estuary advection on the flood does not return the isohalines to uniformity at HW, (d). The possibility of unstable stratification in the lower water column, (d), could lead to complete mixing in the near-bed layer and introduce a tidal asymmetry into the stratification. In the laterally varying case the summation of tidal and density currents, shown separately on (e), produces enhanced flood currents in the main channel and enhanced ebb currents on the shoals. Starting again at HW with uniformly spaced and laterally mixed 18–22 isohalines, (f), then in the absence of mixing, down-estuary advection on the ebb leads to transverse salinity variations at LW, (g). Up-estuary advection on the flood does not return the isohalines to uniformity at HW, (h). The possibility of a mid-channel salinity and density maximum could lead to transverse flow convergence and the formation of an 'axial' convergence front.

also accompanying wind and density-driven) currents. The isohalines can become very distorted when there are strong shears in the currents (Figure A1), which can sometimes lead to the generation of secondary, residual (i.e. subtidal or tidally averaged) flows and associated fronts.

**A2:** The shearing stress, $\tau_z$, in a predominantly longitudinal, horizontal flow dominated by vertical (depth axis) turbulent momentum mixing is often parameterized in terms of the vertical eddy viscosity, $N_z$:

$$\tau_z = \rho N_z \partial_z U$$

where $U$ is the turbulent-mean component of longitudinal velocity, $\rho$ the water density, $z$ the depth coordinate (measured upwards, increasing from bed to surface) and $\partial_z U$ the vertical current shear. The stress will only correlate exactly with the shear if $N_z$ does not vary temporally throughout the tide. Averaging $\tau_z$ and $\partial_z U$ over a tidal cycle gives the vertical distributions of tidally averaged stress and shear, respectively. The vertical flux, $\mathcal{J}_{c,z}$, of a solute, $C$, in a predominantly longitudinal, horizontal flow dominated by vertical turbulent mixing is often parameterized in terms of a vertical eddy diffusivity, $K_{c,z}$:

$$\mathcal{J}_{c,z} = -K_{c,z} \partial_z C$$

**A3:** There are several definitions for the bulk Richardson number, depending on the application. In a three-layer estuary, comprising two well-mixed layers separated by a pycnocline layer that possesses strong gradients and shears, it is defined as:

$$R_{ib} = -g\Delta\rho\Delta z/(\rho_0|\Delta U|^2) = g'\Delta z/|\Delta U|^2$$

where $\Delta\rho$ is the density difference between the upper and lower layers ($\Delta\rho<0$ for stable layering and $\rho_0$ is a reference water density), $\Delta z$ is thickness of the pycnocline layer, $\Delta U$ the difference in turbulent-mean velocity between upper and lower mixed layers, $g$ the gravitational acceleration and $g'$ the reduced gravity.

**A4:** The ' law of the wall ' relates the horizontal turbulent-mean velocity, $U$, at a point above the bed (the ' wall ') to the point's height above the bed, $z$, the shear velocity, $U_\star$, and the hydraulic roughness length, $z_0$:

$$U = (U_\star/\kappa)\ln(z/z_0)$$

where $\kappa$ is von Karman's constant ($\kappa \cong 0{\cdot}41$). The shear stress exerted on the bed by the flow of water, of density $\rho$, is:

$$\tau_z|_{bed} = \rho U_\star{}^2$$

Deviations from the ' law of the wall ' occur not only as a result of water column stability, but also during accelerating and decelerating phases of the tide as well as other situations (e.g. Collins *et al.*, 1998).

**A5:** The tidally averaged (denoted by $\langle\cdot\rangle$) balance of momentum that describes the transverse (across the estuary, $y$) turbulent-mean velocity, $V$, in terms of the longitudinal ($x$) and vertical ($z$) turbulent-mean velocities, $U$ and $W$, and pressure, $P$, is:

$$\langle U\partial_x V + V\partial_y V + W\partial_z V\rangle + f\langle U\rangle = -\langle\rho_0{}^{-1}\partial_y P\rangle + \langle\partial_z(N_z\partial_z V)\rangle$$

where $f$ and $\rho_0$ are the Coriolis parameter and reference density, respectively. The assumption made here (aside from the validity of using the eddy viscosity, $N_z$)[A2] is that the sum of the water's advection and Coriolis accelerations (first two terms in brackets) equals the pressure forcing and vertical shear drag (last two terms, respectively) when averaged over a tidal cycle.

**A6:** The gradient Richardson number is used to describe the interaction of Reynolds stress[A11] with shear and stratification:

$$R_i = -g\partial_z\rho/(\rho_0|\partial_z U|^2)$$

where $\rho$ and $\rho_0$ are the water density and reference density, $g$ the gravitational acceleration and $\partial_z U$ the vertical shear ($z$ upwards) in the turbulent-mean longitudinal velocity.

**A7:** The densimetric Froude number is a physical parameter that governs the stability and behaviour of frictionless, steady state, two-layer flows. Where a topographical feature such as a sill or width constriction acts as a control on the flow, then an inflow Froude number, $F_0$, can be invoked, which is specified in terms of the turbulent-mean flow and topographical properties at the control section. The square of the inflow Froude number, $F_0^2$, is defined by:

$$F_0^2 = Q_0^2/(g'H_0^3B_0^2) = U_0^2/g'H_0$$

where $Q_0$, $U_0$, $B_0$, $H_0$, $g'$ are rate of discharge, section-averaged velocity, width and depth at the sill or constricted mouth and reduced gravity[A3], respectively. The initial frontal system (Plate 1(B)) appears to have been triggered at LW+2·1 h by an inflow Froude Number transition at the neck of the inlet:

$$1{\cdot}0 > F_0^2 = U_0^2/g'H_0 > 0{\cdot}3$$

According to Farmer and Armi (1986), this condition results in the blocking of fresher, surface estuarine waters seaward of the inlet neck. The critical inflow Froude Number, $F_0^2=1$, results in plunging of surface waters at the neck of the inlet (at LW+3·1 h, Plate 1(B)).

**A8:** The internal Froude number for a two-layer flow (e.g. Zhou, 1998) is:

$$F_i^2 = F_u^2 + F_l^2 = U_u^2/g'H_u + U_l^2/g'H_l$$

where $F_u$ and $F_l$ are the upper and lower layer Froude numbers and $U_u$ and $U_l$ are the average, turbulent-mean velocities in the upper and lower layers (of thickness $H_u$ and $H_l$) and $g'$ is reduced gravity[A3]. When $F_i$ becomes supercritical ($F_i>1$) then internal waves cannot travel against the flow and wave amplification and instability may result, leading to strong mixing.

**A9:** Turbulent energy dissipation per unit volume, $\varepsilon$, for isotropic turbulence has the property that it is proportional to the turbulent-mean-squared vertical shear of the longitudinal turbulent velocity and $\mu$, the dynamic viscosity of the turbulent waters (Townsend, 1956):

$$\varepsilon = 7{\cdot}5\mu\langle(\partial_z u)^2\rangle''$$

where $u$ is the turbulent component of longitudinal velocity, $z$ the depth coordinate and $\langle\cdot\rangle''$ a time average over the turbulence (i.e. turbulent mean). A frequently used measure of the turbulent velocity shear, $G$, ($s^{-1}$) is (Dyer & Mannning, 1999):

$$G = (\varepsilon/\mu)^{1/2}$$

**A10:** The turbulent Froude number is a measure of the ratio of the largest possible turbulent scale length, $l_N$, to the active turbulent scale length for the flow, $l_E$:

$$F_r = (l_N/l_E)^{2/3} = 0{\cdot}48R_i^{-1/2}$$

Forced reduction of $l_N$ by, e.g., a physical interface may increase $R_i$[A6] and enhance stability.

**A11:** The along-channel Reynolds stress (i.e. the shearing stress resulting from turbulence[A2]) is the turbulent-mean rate of momentum transport by turbulent currents:

$$\tau_z = -\langle\rho uw\rangle''$$

where $\langle\cdot\rangle''$ is a time average over the turbulence, $\rho$ is the water density and $u$ and $w$ are the turbulent components of longitudinal and vertical velocity, respectively. The shear-generated rate of production of turbulent energy by the working of the turbulent-mean flow against the Reynolds stresses is:

$$P_k = -\langle\rho uw\rangle''\partial_z U$$

Where $\partial_z U$ is the vertical shear in the turbulent-mean longitudinal velocity.

**A12:** Tidal pumping of salt refers to the correlation between tidal variations in salinity and velocity. The instantaneous rate of water discharge through an estuarine section of area $A$ is $Q$, where $Q = A\overline{U}$, in which the overbar denotes a spatial average over the section. The rate of salt transport is $A\overline{U}\cdot\overline{S} + A\cdot\overline{U'S'} = Q\overline{S} + A\cdot\overline{U'S'}$ where the primes denote a spatial deviation from the section average. Expressing this rate of salt transport in terms of the tidally averaged water discharge and its tidally fluctuating part: $Q = \langle Q\rangle + \tilde{Q}$ leads to a relationship for the tidally averaged salt transport:

$$\langle Q\rangle\langle\overline{S}\rangle + \langle\tilde{Q}\tilde{S}\rangle + \langle A\cdot\overline{U'S'}\rangle$$

The first term is the transport due to the tidally averaged flow (e.g. runoff), the second is due to tidal pumping and the third is shear transport. The intra-tidal contributions to the tidal pumping and shear terms for a spring tide in the central Tamar are illustrated in Figure 7(b). In steady state, when the rate at which salt is flushed seaward by the mean flow of water is balanced by the up-estuary transport of salt due to pumping and shear, a longitudinal dispersion coefficient, $D$, is often defined by:

$$-D\langle A\rangle\partial_x\langle\overline{S}\rangle = -\langle Q\rangle\langle\overline{S}\rangle = \langle\tilde{Q}\tilde{S}\rangle + \langle A\cdot\overline{U'S'}\rangle$$

This steady balance is not achieved for the data shown in Figure 7, partly because of non steady conditions and partly because of the errors involved in attempting to measure mean transport, especially $\langle Q\rangle$ (Lane *et al.*, 1997). Estimating $D$ from the sum of pumping and shear gives a value of 120 $m^2\ s^{-1}$, of which 70 $m^2\ s^{-1}$ is due to pumping and 50 $m^2\ s^{-1}$ is due to shear.

**A13:** The Mellor Yamada level 2 (MY2) model represents the vertical eddy viscosity and diffusivity[A2] by:

$$N_z = \varphi_N lq;\ K_z = \varphi_K lq$$

where $\varphi_N$ and $\varphi_K$ are stability functions (functions of $R_i$[A6]), $l$ is a scale length and $q$ the turbulent speed:

$$l = \kappa z(1 - z/H)^{1/2}$$

$$q = (u^2 + v^2 + w^2)^{1/2}$$

where $u$, $v$, $w$ are the longitudinal, transverse and vertical components of turbulent velocity, $z$ and $H$ are height above bed and water depth, and $\kappa$ is von Karman's constant[A4]. Evolution through time ($t$) of the turbulent kinetic energy per unit mass, $k = q^2/2$, may be written:

$$\partial_t k - \partial_z(K_{q,z}\partial_z k) = N_z|(\partial_z U)^2 + (\partial_z V)^2| + K_z(g\partial_z\rho/\rho_0) - q^3/B_1 l$$

in which $U$ and $V$ are the turbulent-mean horizontal velocities, $\rho$ and $\rho_0$ are density and reference density, $g$ is gravitational acceleration and $B_1$ represents the Mellor Yamada constant. The left-hand side of this equation is assumed to be zero in the MY2.0 scheme, so that the right-hand side represents a balance between shear and buoyancy production of turbulent kinetic energy (first and second terms) and dissipation (last term) per unit mass. In MY2.2 models the left-hand side of the equation is retained and the time-dependence is taken into account. The MY2.5 model is a two-equation model that calculates the evolution of both the turbulent kinetic energy and the turbulent

kinetic energy multiplied by the length scale ($kl$), where $l$ is now treated as an unknown to be solved, although there are mathematical difficulties associated with this latter equation (Burchard, 2001b). The $k$–$\varepsilon$ model is essentially the same as MY2.5 except that this second equation for $kl$ is replaced by an equation for the dissipation rate, $\varepsilon$, which once computed is then used to compute the length scale algebraically from $k$.

**A14:** Hearn's adaptation of the Stommel model, which originally applied to thermohaline convection, considers an estuarine basin of length $L$ with mean salinity and temperature $S$ and $T$ and oceanic salinity and temperature (at the estuary mouth) of $S_0$ and $T_0$. The model utilizes the following time-dependent ($t$) equations:

$$\partial_t \Delta T = Q_s/\rho H C_p - 2D\Delta T/L^2$$

$$\partial_t \Delta S = S_0 E/H - 2D\Delta S/L^2$$

$$\text{where } \Delta S = S - S_0 \text{ and } \Delta T = T - T_0$$

and where $Q_s$ is the net rate of surface heating, $C_p$ is specific heat, $E$ is evaporative velocity, $D$ is longitudinal dispersion coefficient[A12] and $H$ the estuary depth. If the ocean saltwater density exceeds, equals, or is less than the estuarine salinity, then the estuary is termed ' classical ', ' neutral ' or ' inverse ', respectively.